Rydberg atoms with Black-body radiation with microwaves Rydberg-atom – Rydberg-atom collisions

(Use of T.F. Gallagher's lectures)

Blackbody radiation

The Rydberg atoms are very sensitive to the environment

Effect of 300K blackbody radiation: both redistributes the Rydberg levels and shifts the energy levels.

<u>The former is the more important.</u>

300K blackbody radiation is important for Rydberg states because:

They have transitions with large matrix elements and low frequencies.

Molecules have similar rotational frequencies,
but the matrix elements are smaller.

The energy density of 300K black body radiation
(important for the energy shifts)

$k_B T = 1/40$ eV
$= 200\ cm^{-1}$

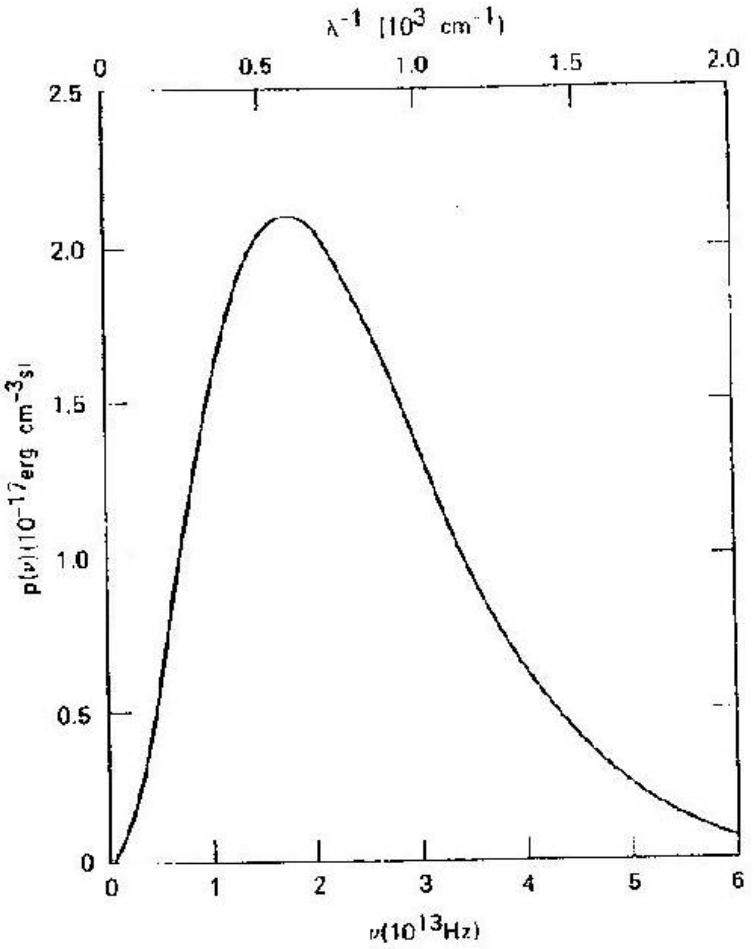

Fig. 5.1 Energy density $\rho(\nu)$ as a function of frequency ν at 300 K (from ref. 5).

The photon occupation number vs frequency at 300K
(important for the redistribution)

$$\bar{n} = \frac{1}{e^{\omega/kT} - 1}$$

For ω<<kT

$$\bar{n} = \frac{kT}{\omega}$$

At 300K kT= 200 cm^{-1}

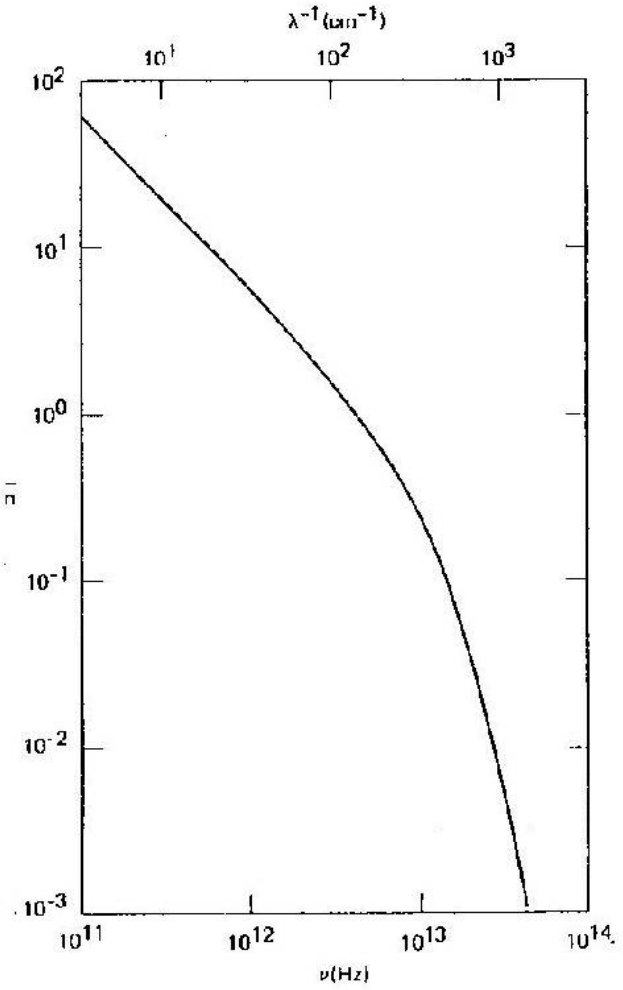

Fig. 5.2 Occupation number $\bar{n}$ as a function of frequency ν at 300 K (from ref. 5).

Spontaneous emission rate (Einstein A coefficient) for the nℓ to n'ℓ' state

$$A_{n'\ell',n\ell} = \frac{4e^2\omega^3{}_{n'\ell',n\ell}}{3\hbar c^3} \cdot \frac{\ell_>}{2\ell+1} \cdot \left|\left\langle n\ell \left| r \right| n'\ell' \right\rangle\right|^2$$

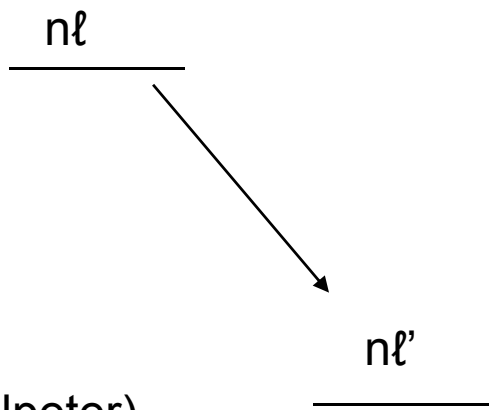

$$A_{n'\ell',n\ell} = \frac{4\alpha^3\omega^3{}_{n'\ell',n\ell}}{3} \cdot \frac{\ell_>}{2\ell+1} \cdot \left|\left\langle nl \left| r \right| n'\ell' \right\rangle\right|^2$$

Using the average oscillator strength (see Bethe and Salpeter)

$$\bar{f}_{n'\ell',n\ell} = \frac{2\omega_{n'\ell',n\ell}}{3} \cdot \frac{\ell_>}{2\ell+1} \left|\left\langle nl \left| r \right| n'\ell' \right\rangle\right|^2$$

$$A_{n'\ell',n\ell} = 2\alpha^3\omega^2_{n'\ell,n\ell} \left| \bar{f}_{n'\ell',n\ell} \right|$$

if the nℓ' state lies below the nℓ state, otherwise it vanishes

The black body transiton rate is

$$K_{n'\ell',n\ell} = \bar{n} A_{n'\ell',n\ell}$$

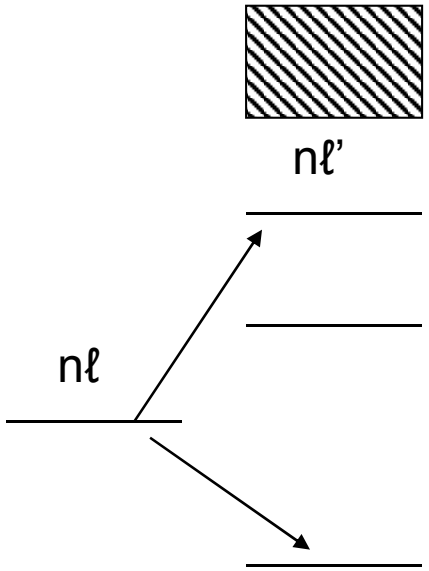

The blackbody radiation can also photoionize the atoms,
it is just the continuation of the photoexcitation rate across the limit.

$$\Gamma_{\varepsilon\ell',n\ell} = \int_{1/2n^2}^{\infty} \frac{dK}{d\varepsilon_{\ell'}} \cdot d\varepsilon_{\ell'} = \int_{1/2n^2}^{\infty} 2\bar{n}\,\alpha^3 \omega^2_{\varepsilon\ell',n\ell} \; \frac{d\bar{f}}{d\varepsilon_{\ell'}} \cdot d\varepsilon_{\ell'}$$

The 0 K decay rate is

$$\frac{1}{\tau} = \sum_{n'\ell'} A_{n'\ell',n\ell}$$

The black body decay rate of the nℓ state is

$$\frac{1}{\tau_{bb}} = \sum_{n'\ell'} K_{n'\ell',n\ell} + \sum_{\ell'} \int_{1/2n^2}^{\infty} \frac{dK_{\varepsilon\ell',n\ell}}{d\varepsilon_{\ell'}} \cdot d\varepsilon_{\ell'}$$

The total decay rate is

$$\frac{1}{\tau^T} = \frac{1}{\tau} + \frac{1}{\tau_{bb}}$$

Approximate sum rule

If most of the black body transition rate comes from transitions with ω<<kT, Then we use

$$\bar{n} = \frac{kT}{\omega}$$

To write (see Bethe and Salpeter for the summation, page 257)

$$\frac{1}{\tau_{bb}} = 2\alpha^3 kT \sum_{n'\ell'} \omega_{n'\ell',n\ell}\, \bar{f}_{n'\ell',n\ell}$$

$$\frac{1}{\tau_{bb}} = 2\alpha^3 kT \cdot \frac{2}{3n^2} = \frac{4\alpha^3 kT}{3n^2}$$

There is no ℓ dependence!

At n=20 and 300 K this gives a rate of 3×10^4 s^{-1}

Redistribution of population is the most important effect.

Example: the Na 18s state

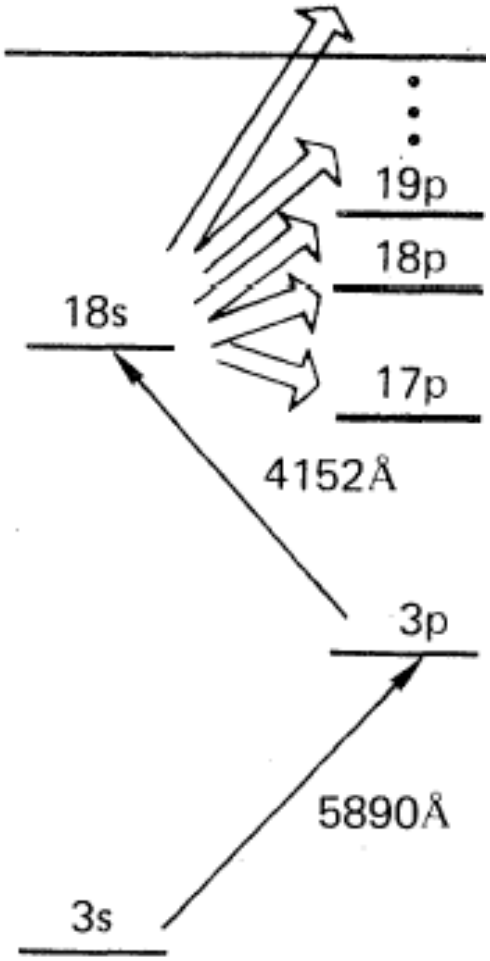

Na 18s to n'p spontaneous and black body transition rates

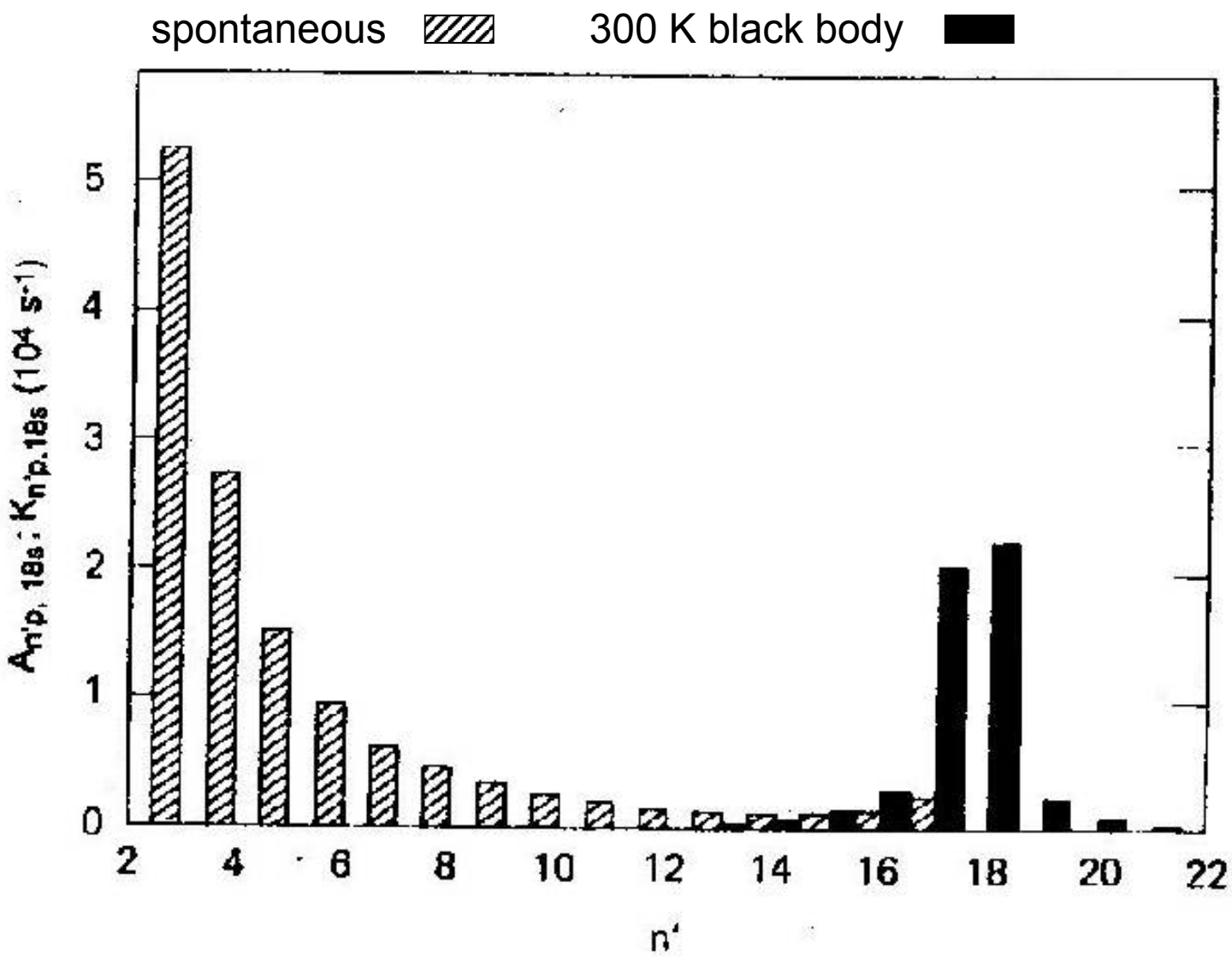

Na n=18 ℓ=17 spontaneous and 300K black body transitions

spontaneous ▨ 300K black body ■

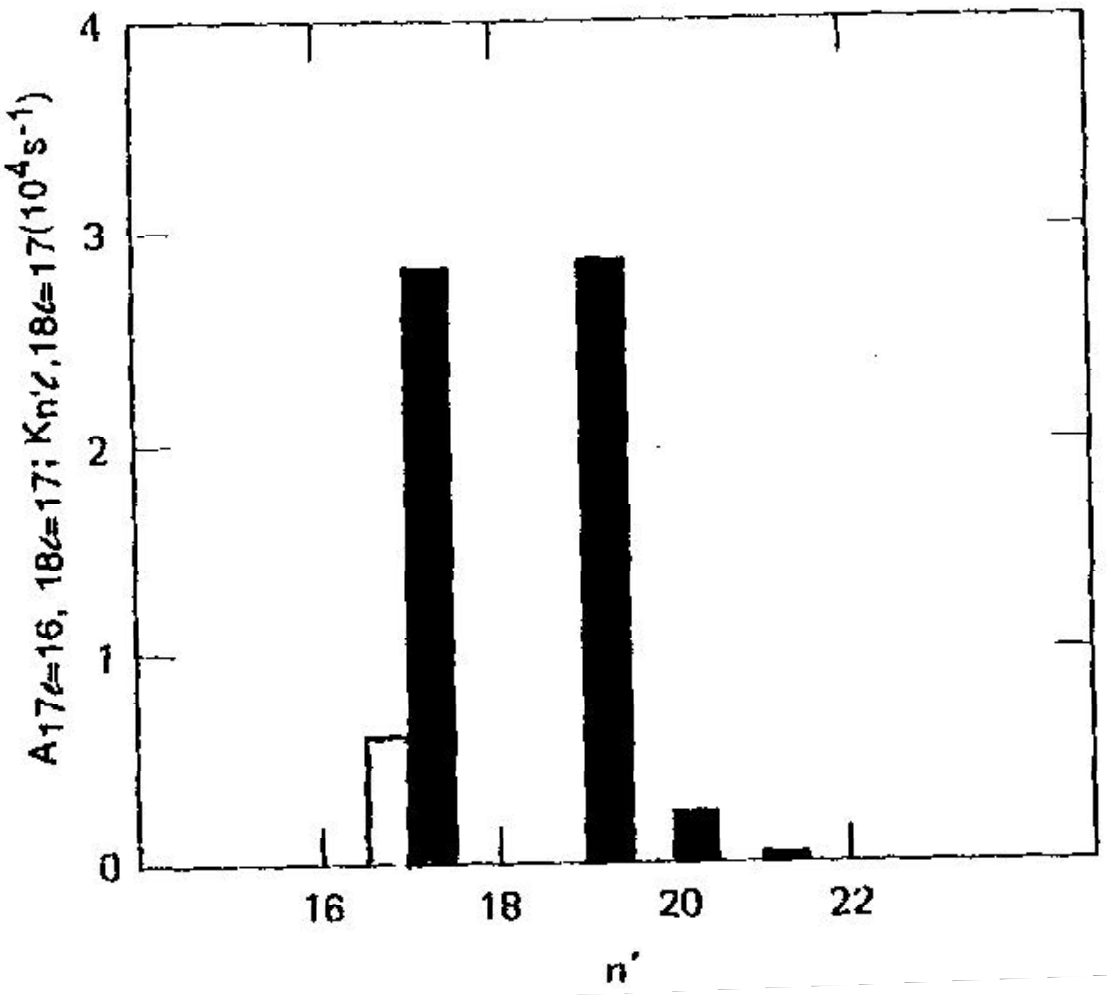

Redistribution of population is the most important effect.

Example: the Na 18s state

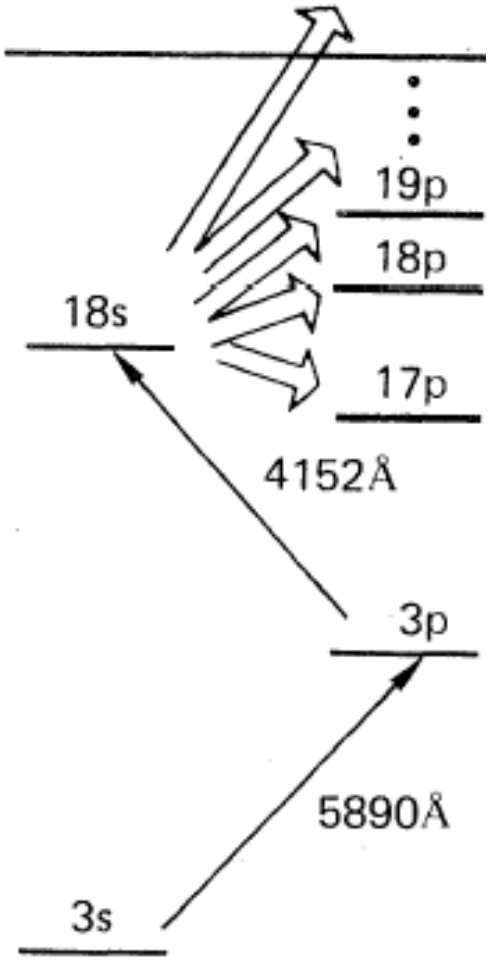

0 K decay rate	1.59×10^6 /s
18s→18p	2.28×10^4 /s
18s→17p	2.14×10^4 /s
300 K decay rate	2.08×10^5 /s
Total bb rate (approximate)	4.0×10^4 /s

Measurement of the lifetime of the Na 18s state

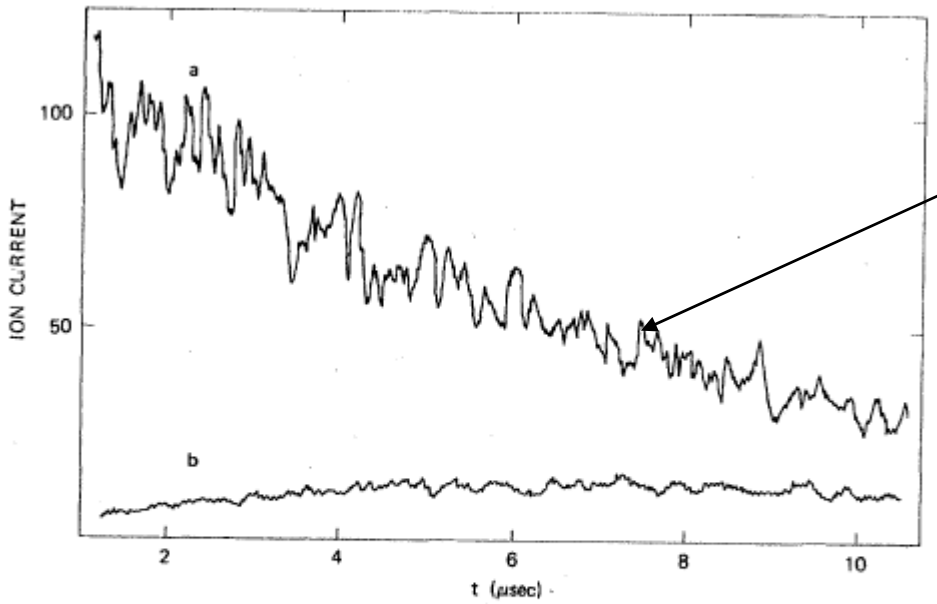

FIG. 5. Observed time dependence of the ionization signal following the initial population of Na 18s state with an ionizing field of (a) 4.85 and (b) 4.14 kV/cm.

1.28×10^5 /s
Slower than the 0K rate

Ionizes 17p and above

Ionizes 18p and above

Superradiant cascade in Rb Rydberg states after population of the 12s state (experiment in a cell)

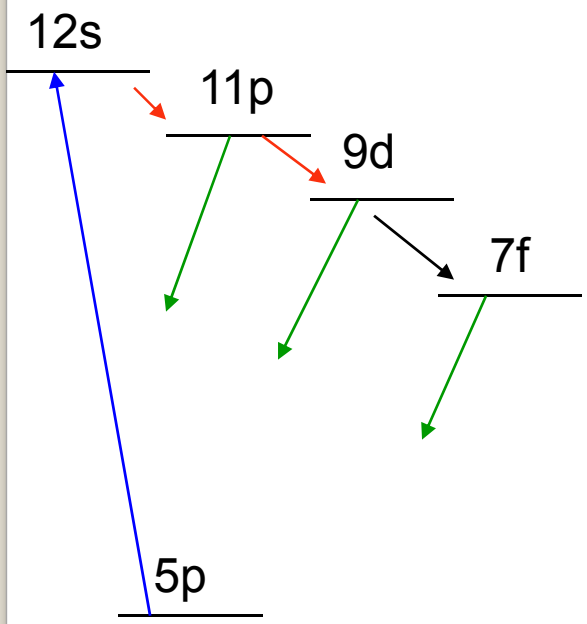

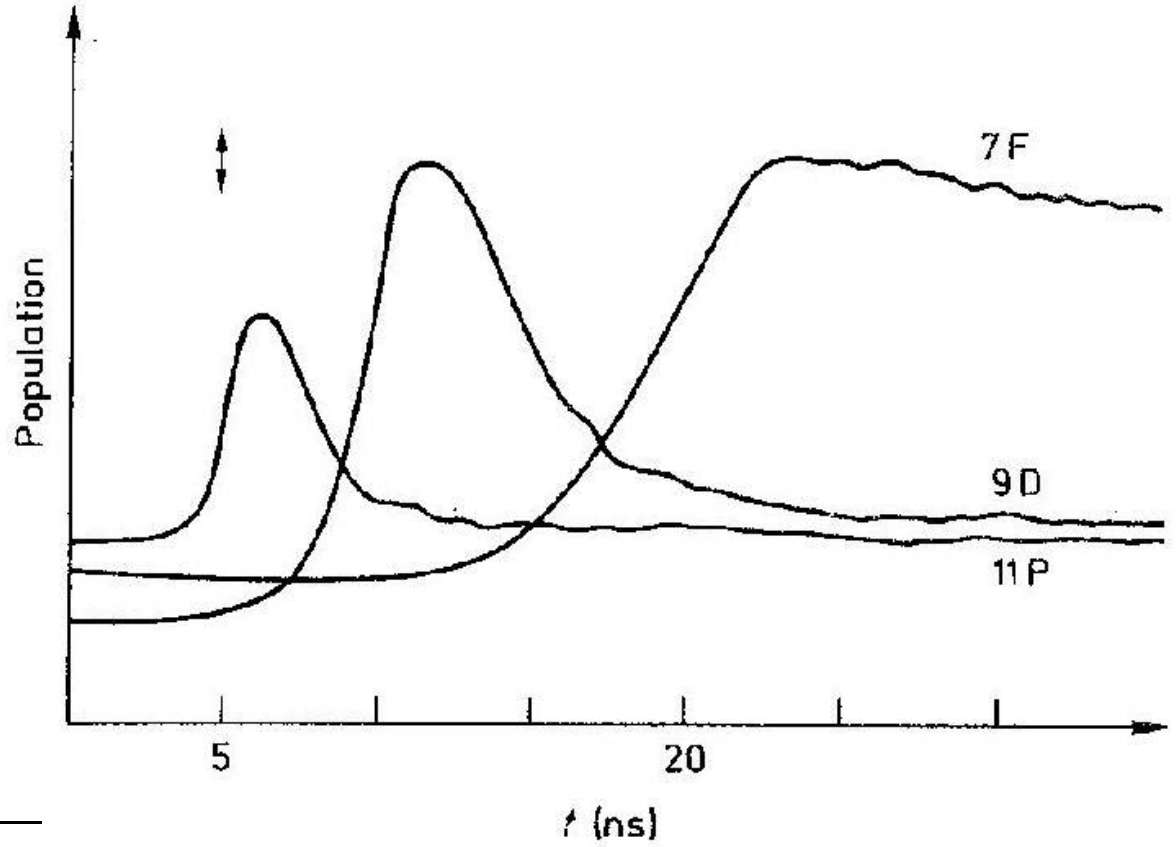

Observed by fluorescence detection

Gounand et al

Photoionization by black body radiation

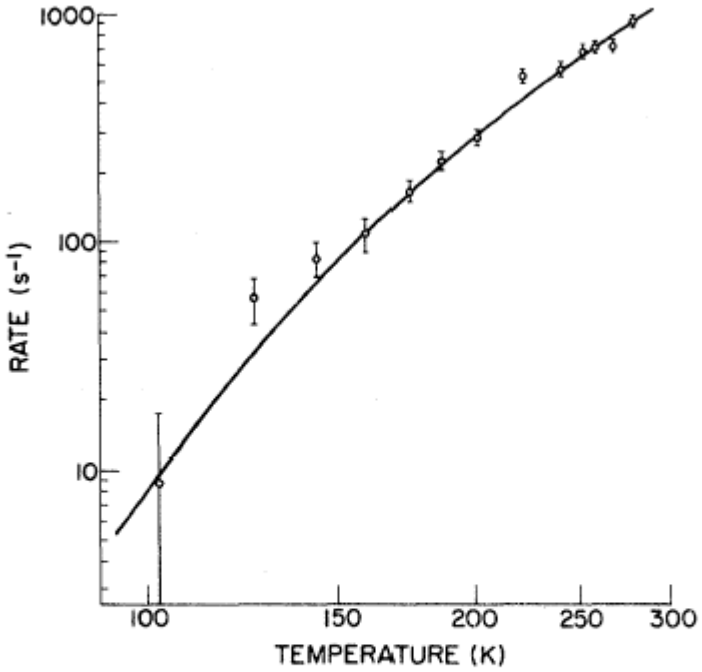

FIG. 1. Blackbody-induced photoionization rate vs temperature for the 17*d* state in Na. Scales are logarithmic. Solid line represents our calculated values. Experimental points were normalized to the calculated value at 300 K.

Spencer et al

Level shifts due to the off resonant field Ecosωt

$$\Delta W = \sum_{n'\ell'} \frac{\left|\langle n'\ell'|z|n\ell\rangle\right|^2 F_z^2 \omega_{n'\ell',n\ell}}{2\left(\omega_{n'\ell',n\ell}^2 - \omega^2\right)}$$

In the high frequency limit, $\omega >> \omega_{n'\ell',n\ell}$, we can write

$$\Delta W = \frac{F_z^2}{-2\omega^2} \sum_{n'\ell'} \left|\langle n'\ell'|z|n\ell\rangle\right|^2 \omega_{n'\ell',n\ell}$$ (an oscillator strength sum)

$$\Delta W = \frac{F_z^2}{-2\omega^2} \cdot \frac{1}{2} = \frac{F_z^2}{4\omega^2}$$

This is the time average kinetic energy of a free electron in the field.

The high frequency field adds a fast oscillation to the electron's orbit.

E=0

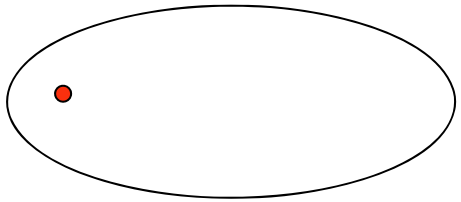

Ecosωt

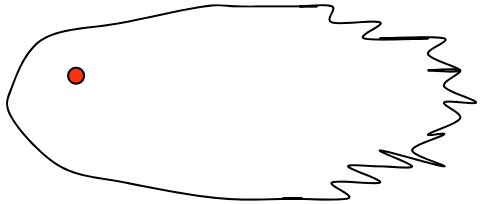

If we replace the monochromatic field by the black body field, we replace E^2 by

$$\int_0^\infty \frac{E_\omega^2 d\omega}{4\omega^2}$$

And we obtain the blackbody energy shift

$$\Delta W = \frac{\pi\alpha^3 (kT)^2}{3}$$

At 300K this shift is 2.2 kHz, which is independent of n and ω and not very big.

Measurement of the bb shift by Holberg and Hall

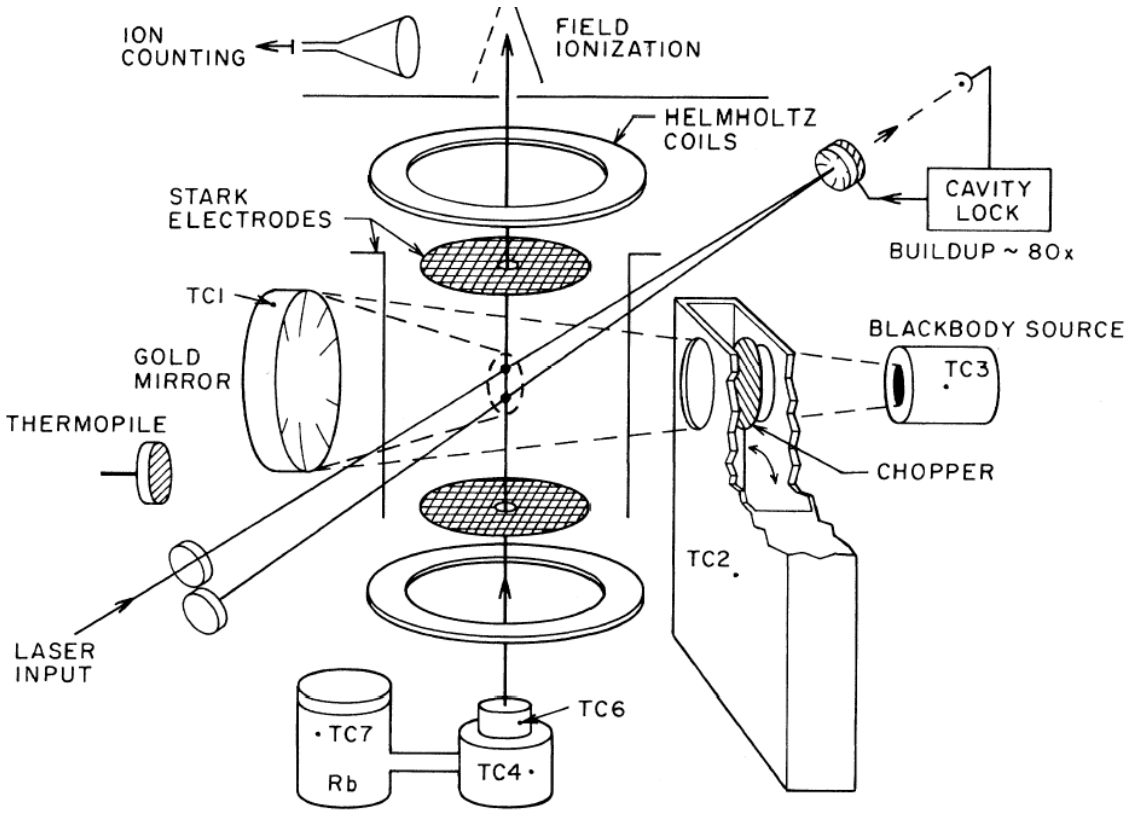

FIG. 1. Schematic of apparatus. A Rb atom in the beam (vertical arrow) may interact twice with the folded intracavity field of the "buildup" resonator located inside the vacuum. Excited Rydberg population is quenched by field ionization to yield an ion count. The blackbody thermal radiation is chopped and focused onto the laser/atom interaction region. Several thermocouples (TC) monitor relevant temperatures.

Vary source temperature
Observe frequency shift
Of excitation

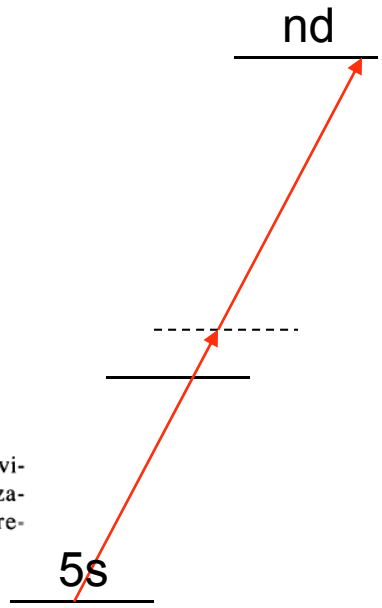

Observed shift agrees with the model presented earlier.

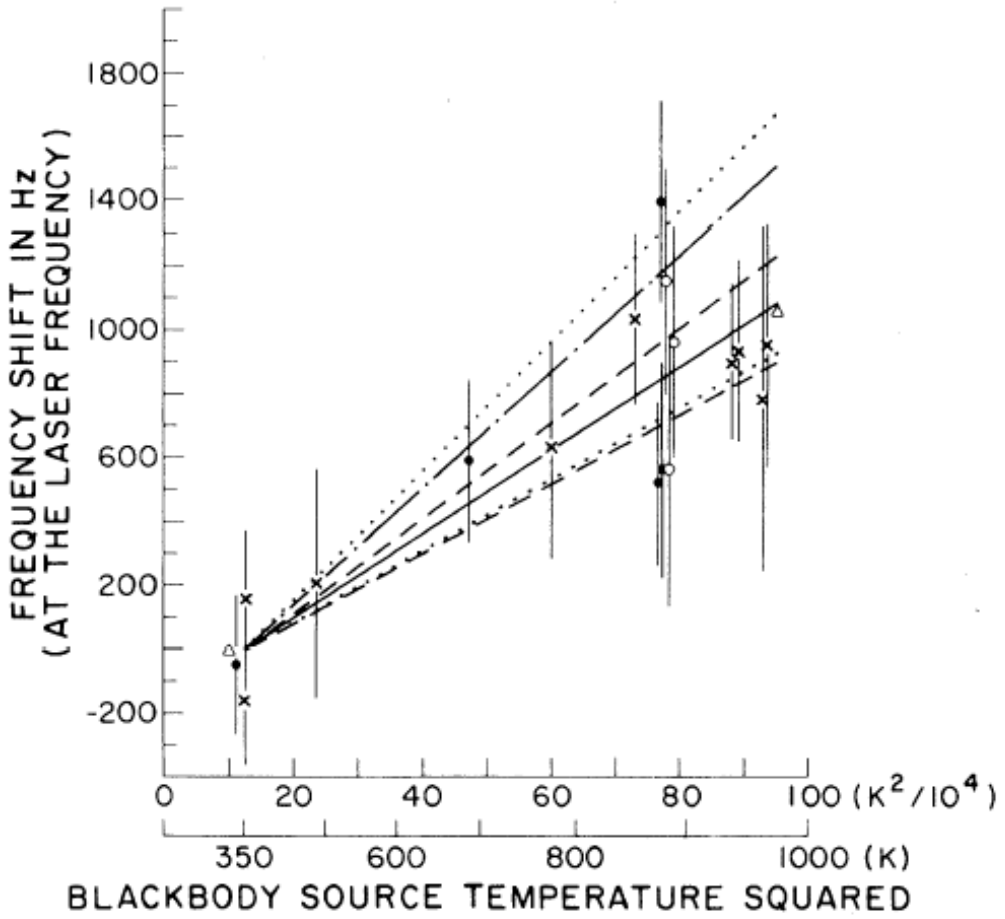

FIG. 4. Temperature dependence of measured thermal-radiation-induced energy-level shift. Points and error flags represent measured values, with best-fitting straight solid line; error limit on experimental fit denoted by dashed lines; theoretical prediction of Eqs. (1) and (2) calculated for our experimental situation (dot-dashed lines) with unsymmetrical error limits (dotted line) of $^{+10}_{-30}$%. The principal uncertainty is the location of the effective atom beam relative to the focus of the BB radiation.

In the Rydberg states it is the population redistribution which is important.
The rates are linear in T.

In other systems, like atomic clocks, it is the frequency shift which is important

Rydberg atoms in microwaves

Micowave ionization
Multiphoton processes

We will the evolution of the electric field from a static field (Stark effect), a quasi-static field (electric field ionization, Landau-Zener transition), a electro-magnetic fied

Motivations

- Microwave ionization of hydrogen
- Microwave ionization of alkali
- Connection between Landau-Zener transition and multiphoton processes
- Photoionization by microwaves

Landau-Zener transition

A two-level transition

Photoionization

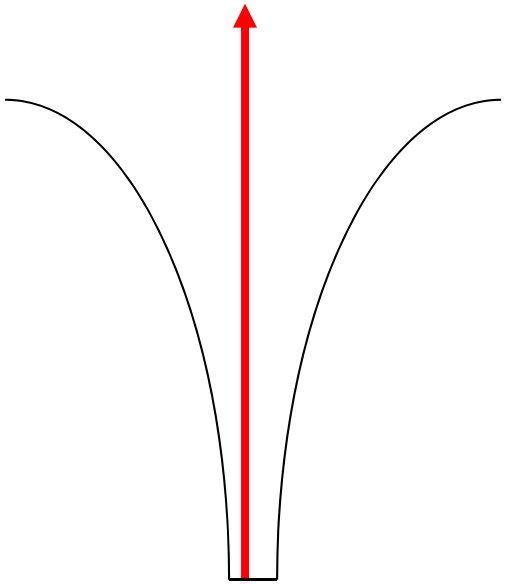

hv> Ionization Potential

Field Ionization

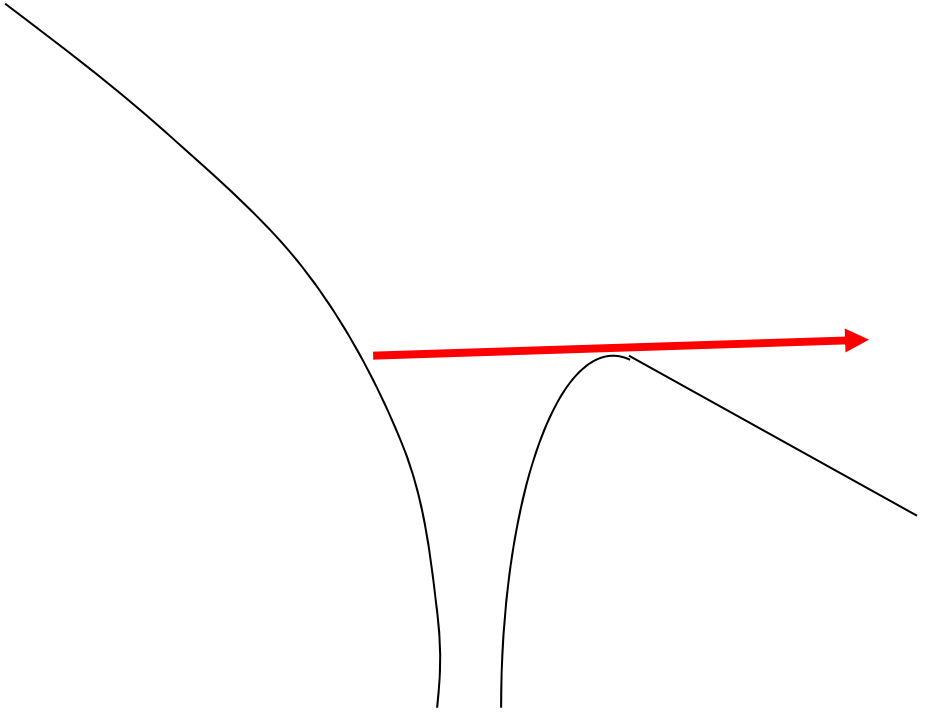

$E>1/16n^4$

Multiphoton Ionization

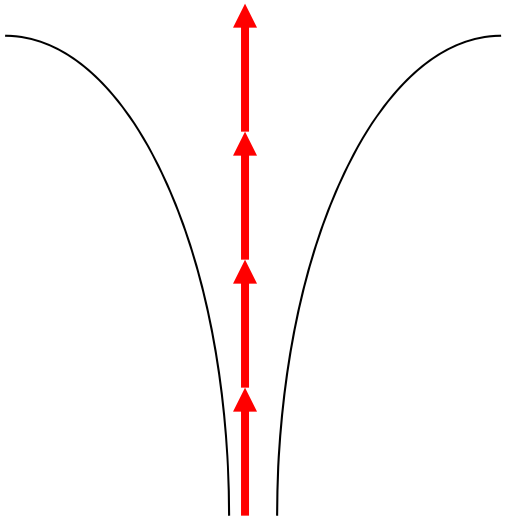

nhv>I.P. high intensity

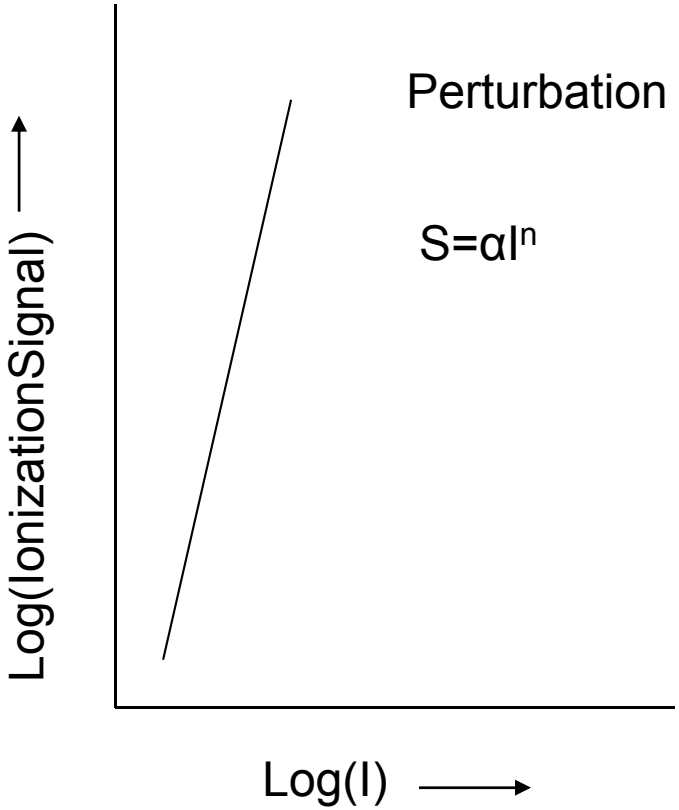

$S=I^n$ Plotted on a linear scale

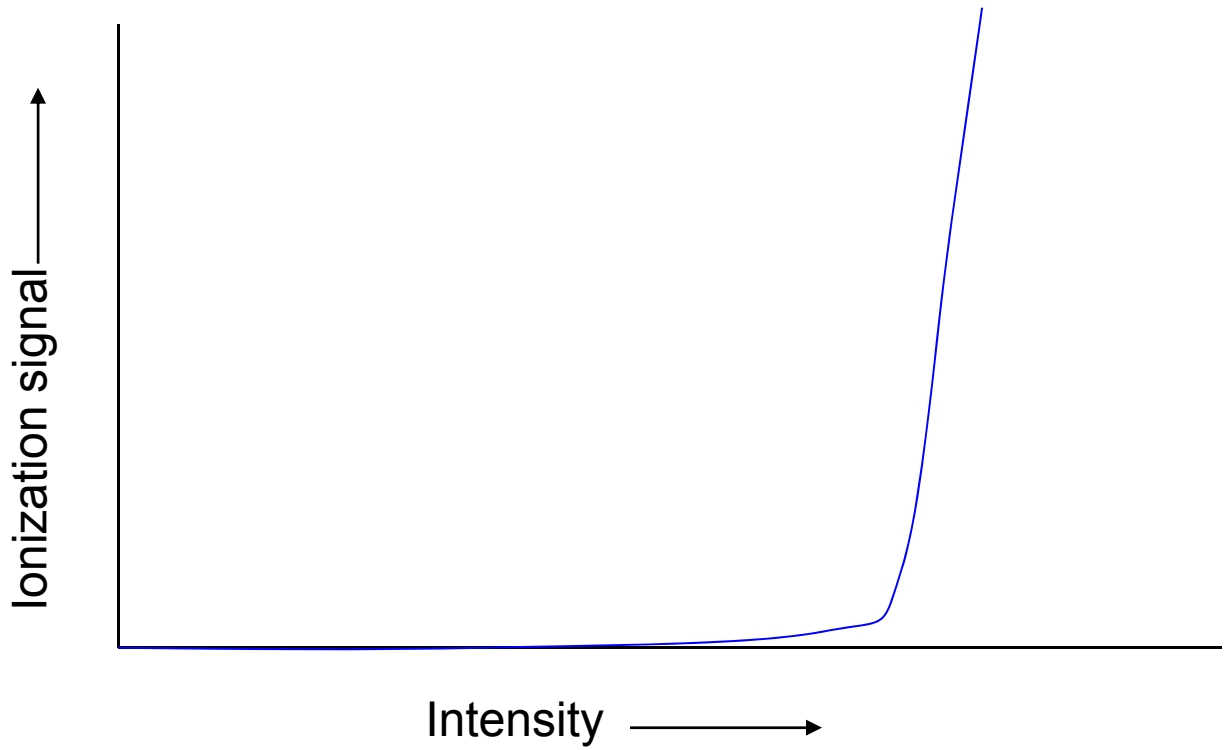

Laser multiphoton experiments are done with focused, pulsed lasers
The laser focus defines the interaction volume.
The laser field is inhomogeneous in space and time.

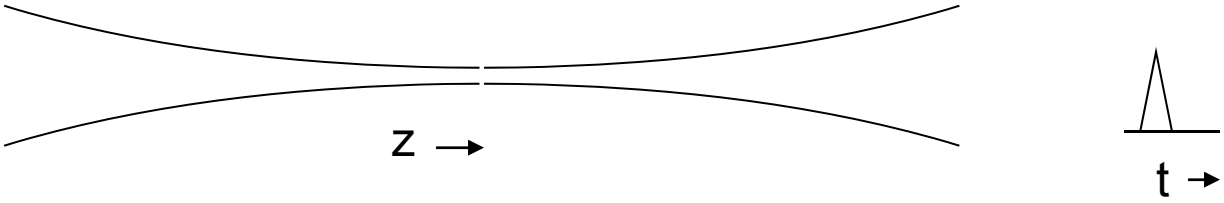

The atom field interaction is μE.
In the laser experiments E is big and μ is small.
In the Rydberg atom μ is big, and E is small.

Rydberg binding energies are small, so we use microwaves.

The samples of atoms are small compared to the microwave wavelength ,~ 1 cm, so all the atoms see the same field.

Ionization of Rydberg atoms
by linearly polarized microwave fields

Field ionization ⟷ Multiphoton ionization ⟷ Photoionization

What, if any, are the connections?

Again, hydrogen and the alkalis are different!

Pioneering Experiments of Bayfield and Koch with hydrogen

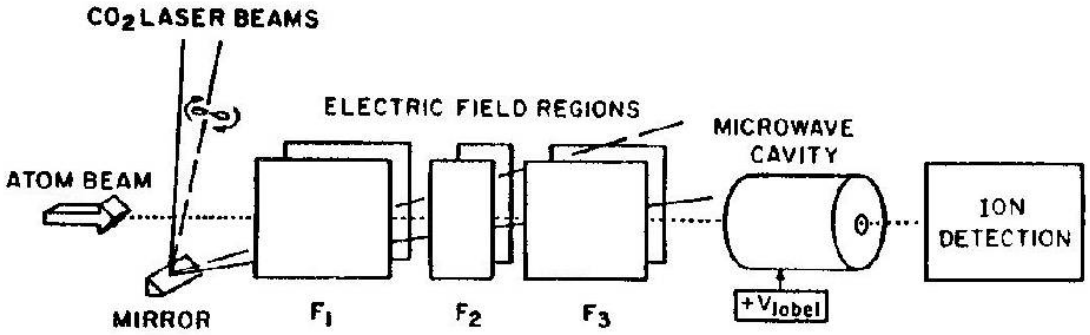

Fig. 10.1 Schematic drawing of a fast beam apparatus. A fast atomic beam enters from the left and is excited sequentially by two different CO_2 lasers in electric field regions F_1 and F_3, respectively. F_2 avoids a zero field region between them. Ions produced by highly excited atoms being ionized in the biased microwave cavity are energy selected and detected by a Johnston particle multiplier (not shown). The output signal is detected in phase with the mechanically chopped F_1 laser beam (from ref. 3).

Measure the ionization fraction of the n=65 H atoms passing through
A microwave or rf cavity as a function of the field strength

H n=65 ionization vs field amplitude for three frequencies

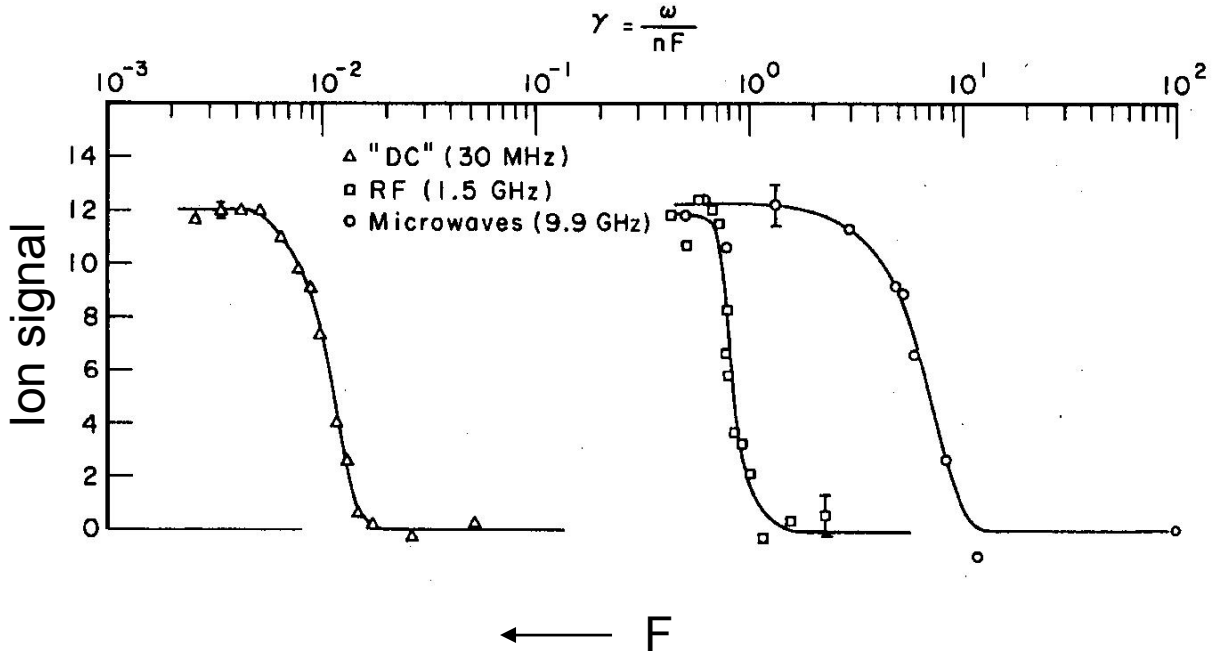

Ionizing fields for n=65

30 MHz	$E=1/9n^4$
1.5 GHz	$E=1/9n^4$
9.9 GHz	$E<1/9n^4$

Later experiments showed that what was important was the ratio of the microwave frequency ω to the $\Delta n=1/n^3$, or classical orbital, frequency. More generally, the problem exhibited classical scaling.

Accordingly the scaled variables below are often used.

Scaled field $F_0 = Fn^4$

Scaled frequency $\Omega_0 = \omega n^3$

Quantum picture of hydrogenic ionization

Mechanism

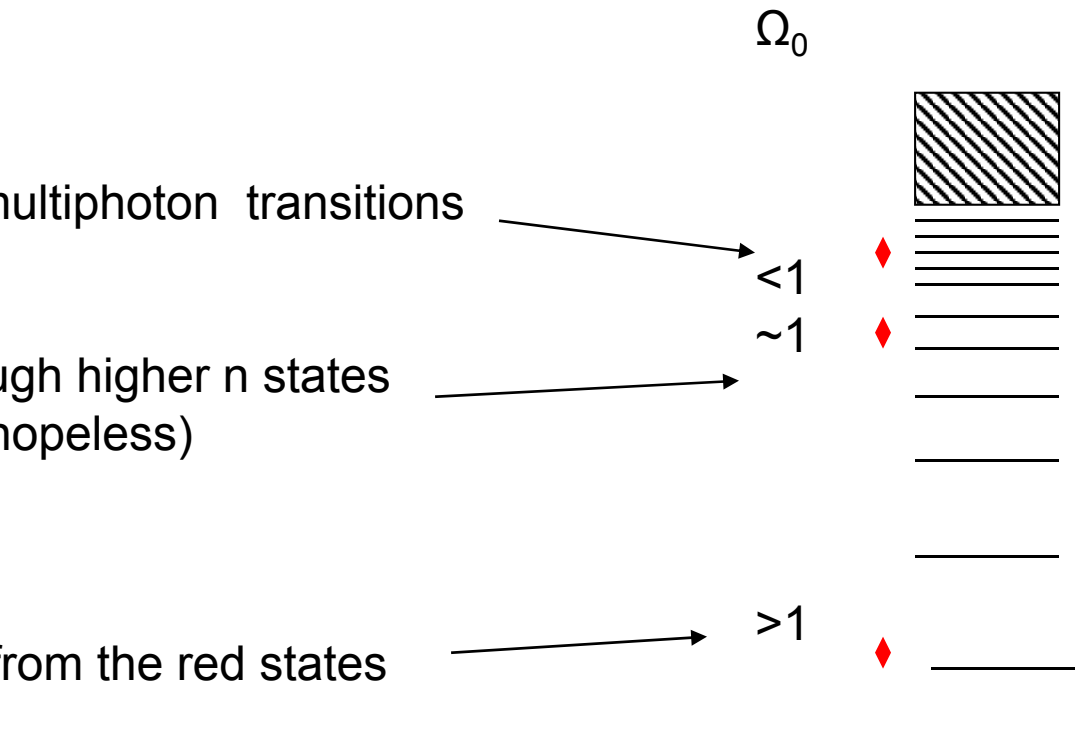

Alkali atoms are different at low scaled frequencies

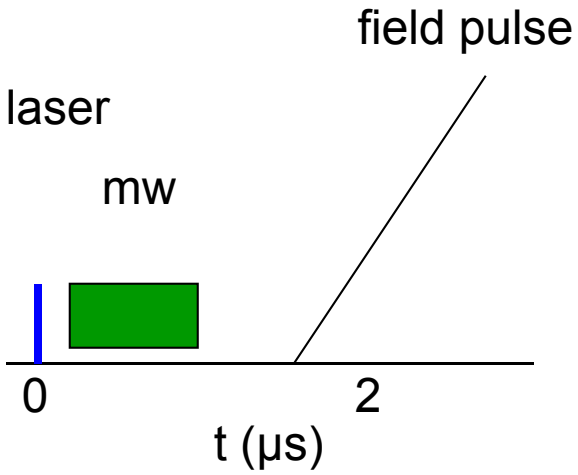

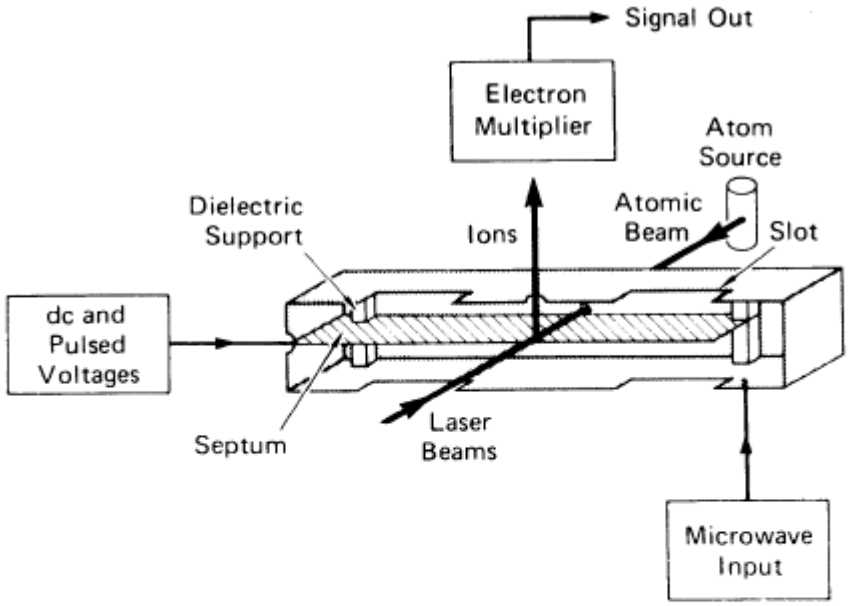

FIG. 3. Main features of the atomic-beam apparatus, the atomic source, the microwave cavity, and the electron multiplier. The microwave cavity is shown sliced in half. The copper septum bisects the height of the cavity. Two holes of diameter 1.3 mm are drilled in the side walls to admit the collinear laser and Na atomic beams, and a 1-mm hole in the top of the cavity allows Na^+ resulting from a field ionization of Na to be extracted. Note the slots for pumping.

Pillet et al

Na 20s

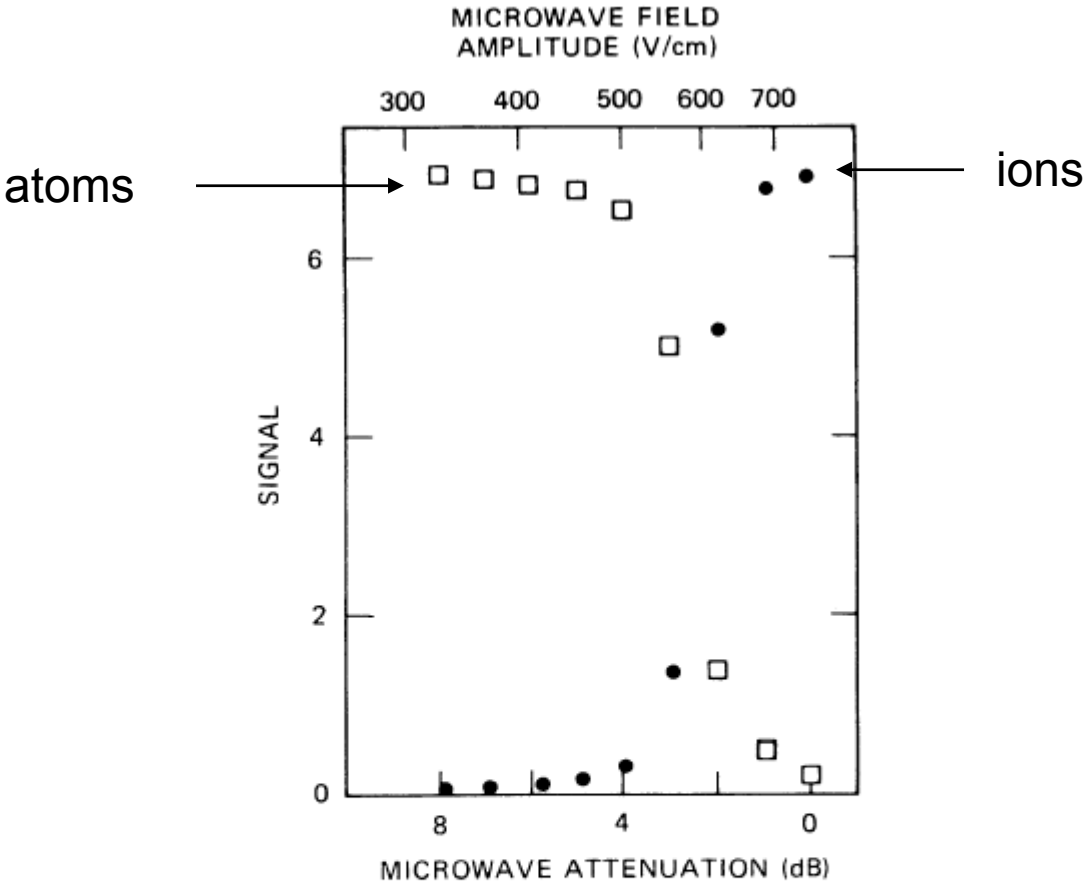

FIG. 5. Field-ionization signal (●) and microwave-ionizatic signal (□) for the Na 20*s* state showing the ionization threshol as a disappearance of the field-ionization signal or the appea ance of the microwave-ionization signal with increasing m crowave power (decreasing attenuation). For convenience th microwave-field amplitude is also given. The signal is given i arbitrary units.

Na m=2 states ionize like hydrogen
$E=1/9n^4$

m=0,1 states ionize near the Inglis-Teller field
$E=1/3n^5$

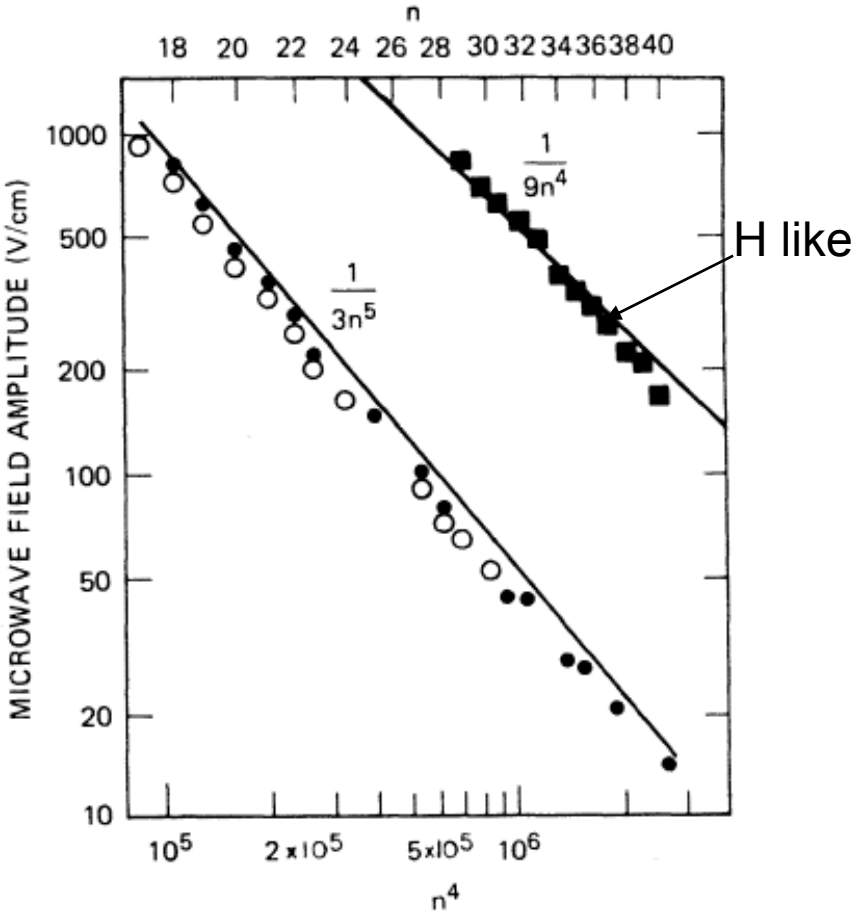

FIG. 8. Logarithmic plot of the ionization-threshold fields for the Na s and d states. s states (○), d states $|m|=0,1$ (●), and d states $|m|=2$ (■). We have plotted the $(n+1)s$ states and nd states as both having quantum number n. We also show for reference the lines $1/3n^5$ and $1/9n^4$ which corespond to commonly encountered dependences of field-ionization thresholds. The ±8% uncertainty corresponds to the size of the s data.

Path in a mw field diabatic

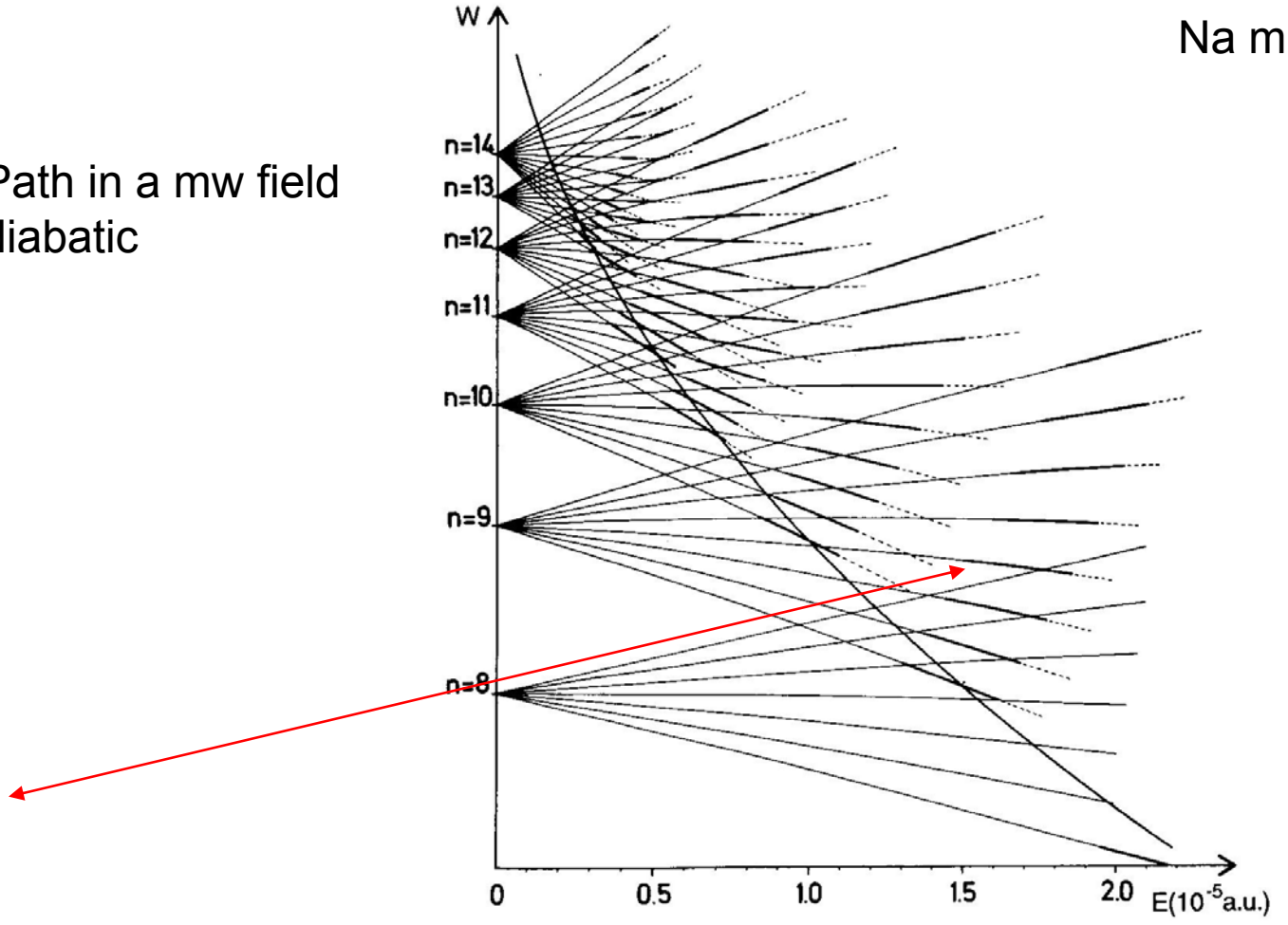

Na m>2

Luc Koenig

Path in the mw field
Partially adiabatic

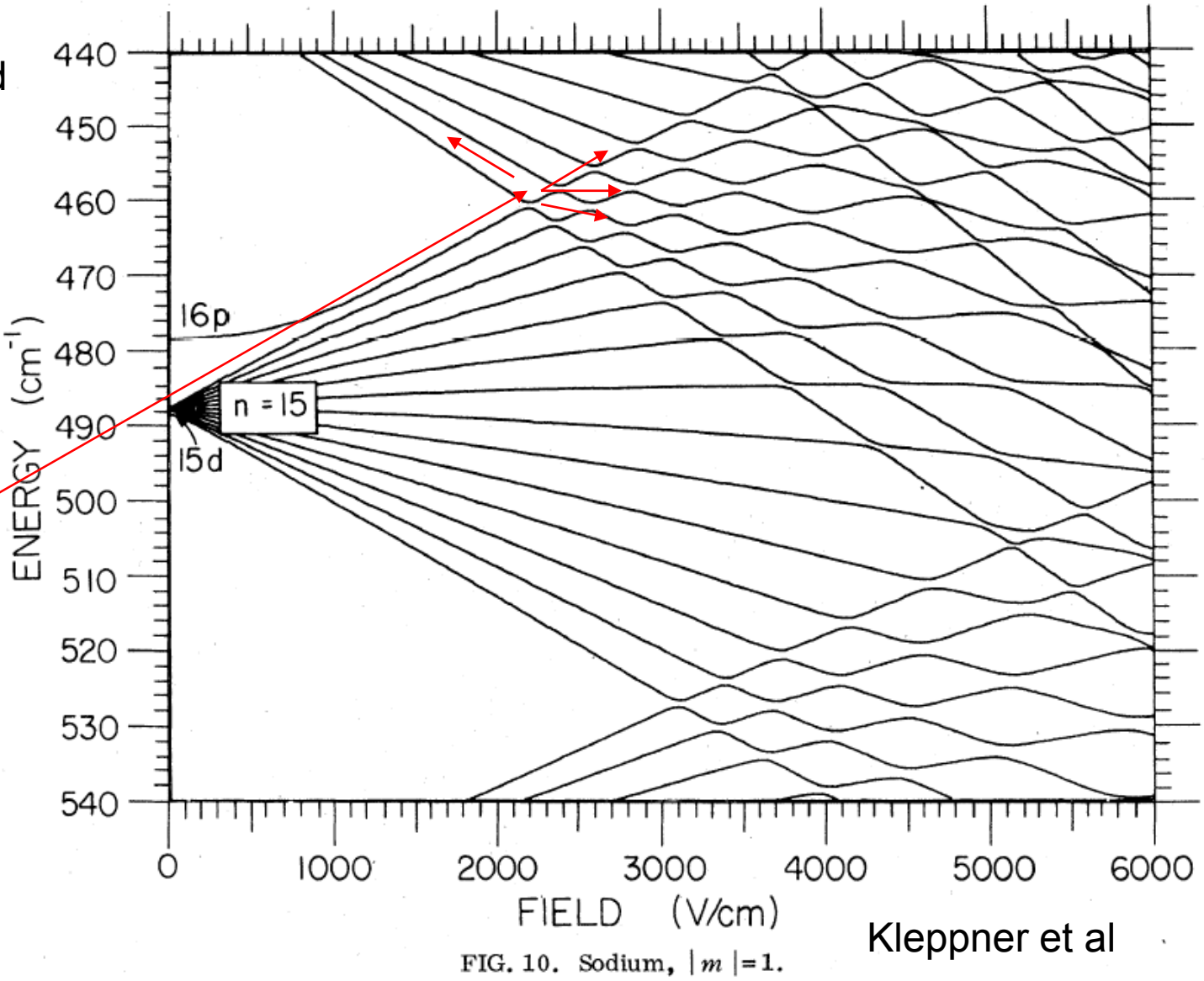

FIG. 10. Sodium, $|m|=1$.

Kleppner et al

The atoms make a Landau Zener transition at the avoided crossing between the extreme n and n+1 Stark levels

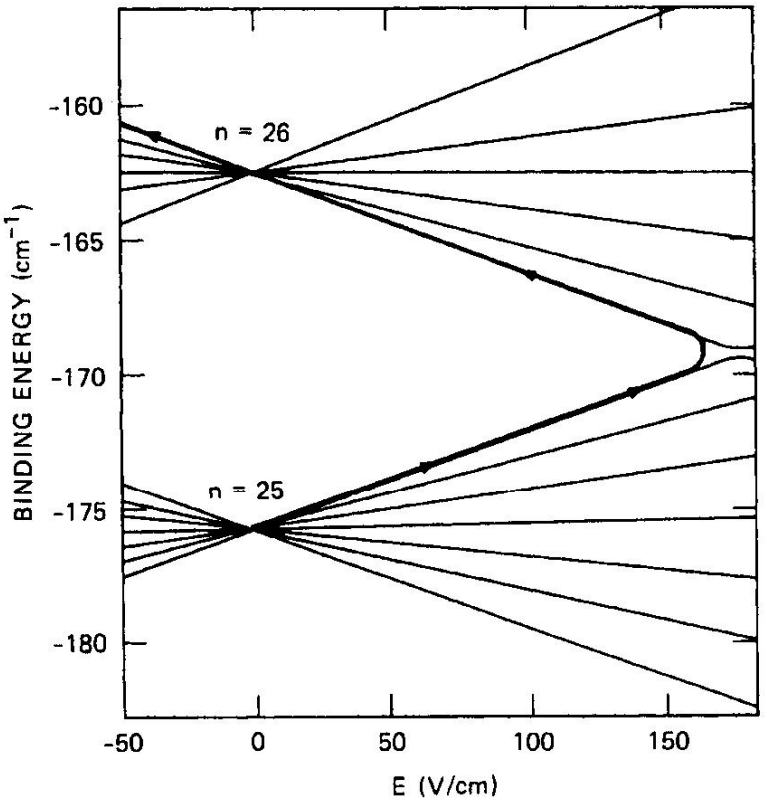

FIG. 1. Schematic diagram of the Landau-Zener description of the $n = 25$ to $n = 26$ transition in Na. Some Na energy levels in an electric field are shown, and the path followed by an atom is shown by the bold line which indicates the Landau-Zener transition at the intersection of the Stark manifolds.

Ionization occurs by a sequence of Landau Zener transitions

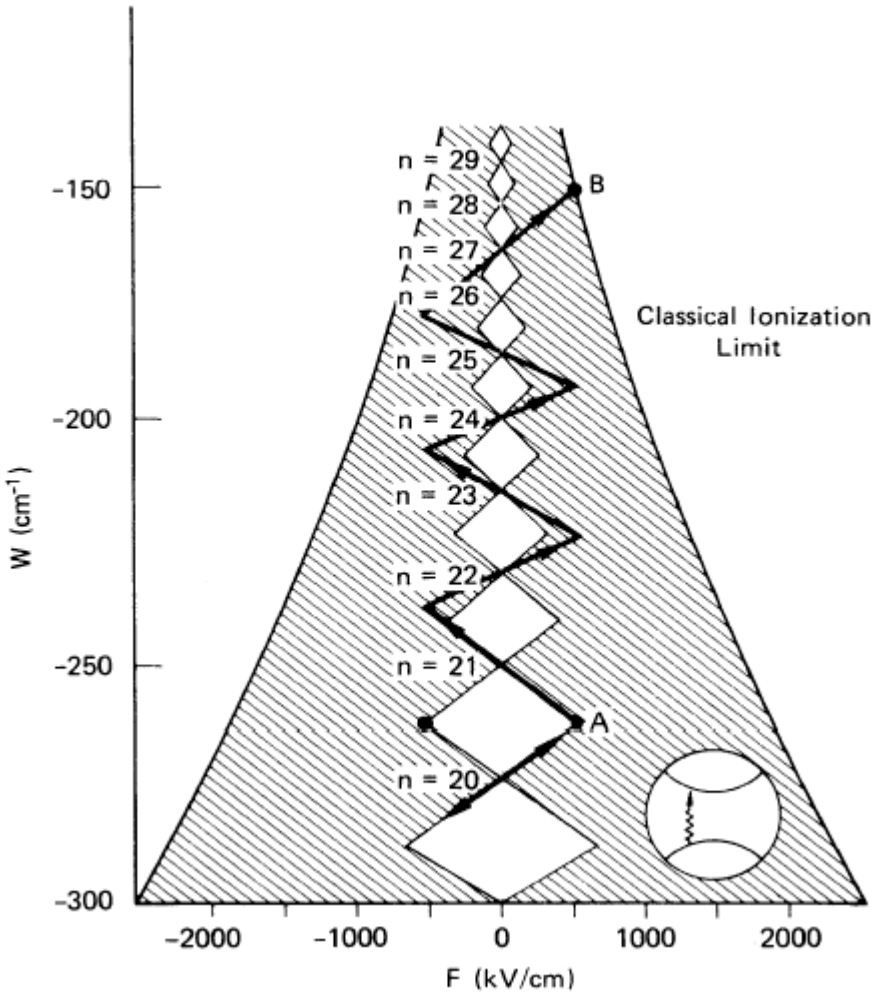

At higher n, or scaled frequency approaching 1 alkali aoms begin to look like H

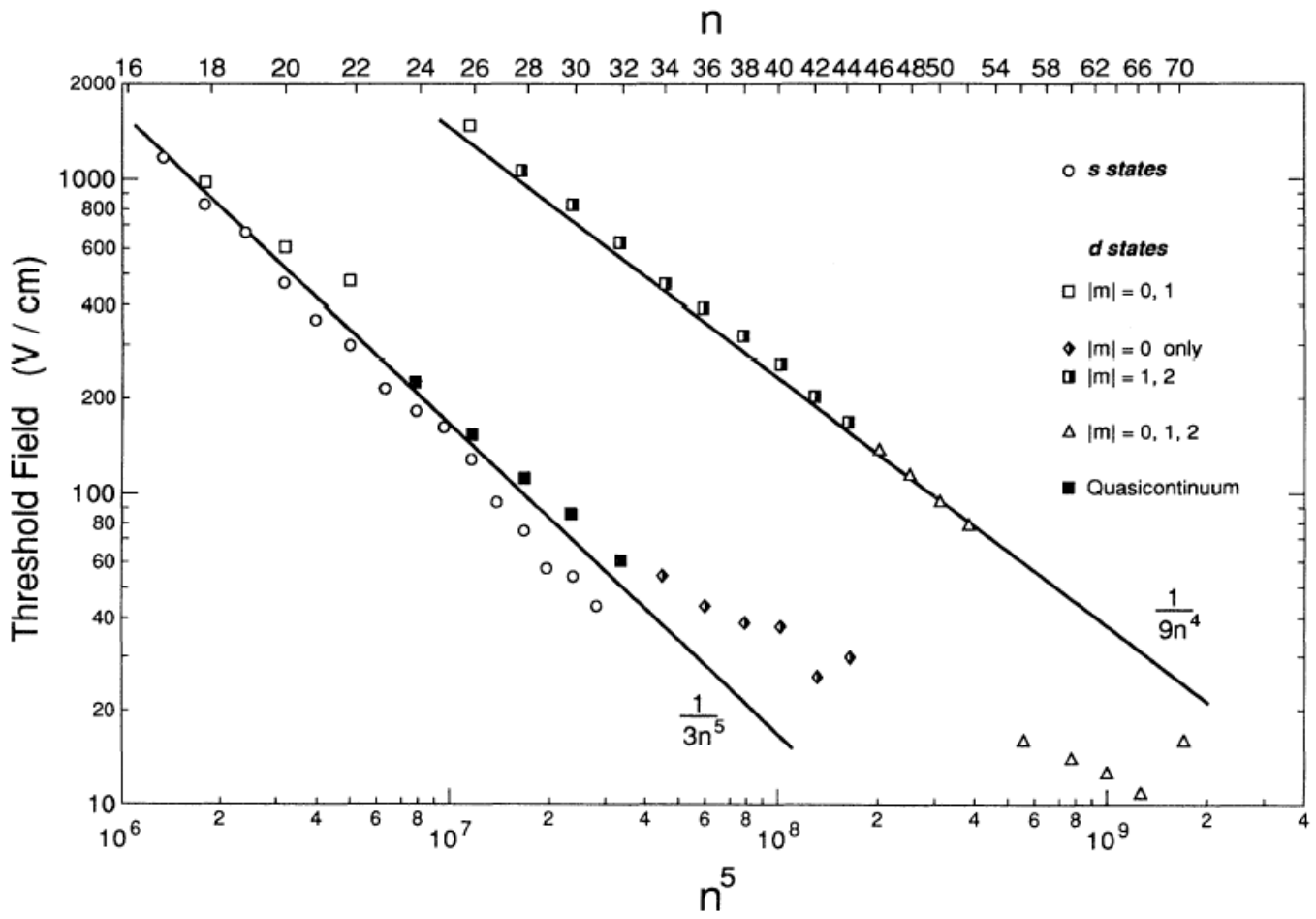

FIG. 19. Li 4-GHz threshold fields for *ns* states and *nd* states. Shown also are the field dependences $1/3n^5$ and $1/9n^4$.

Comparing hydogen, sodium, and lithium

The avoided crossings scale as $1/n^4$ and become too small to be useful in alkalis.

Thus the difference between H and everything else disappears as Ω_0 approaches 1

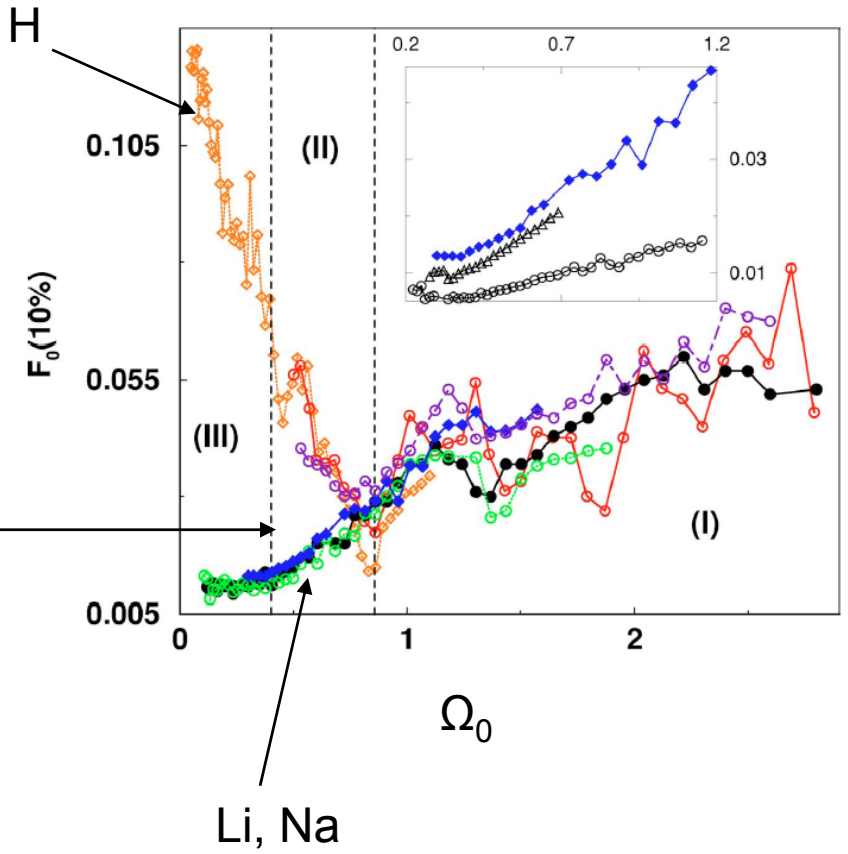

The explanation of the $1/3n^5$ ionization is in terms of Landau-Zener transitions in a time varying field.
What does this have to do with photon absorption?

Lets examine an isolated avoided crossing

The K (n+2)s to n,3 transition
(18s to 16,3)

Varying the static field changes the energy separation and the microwave field required to reach the crossing field.

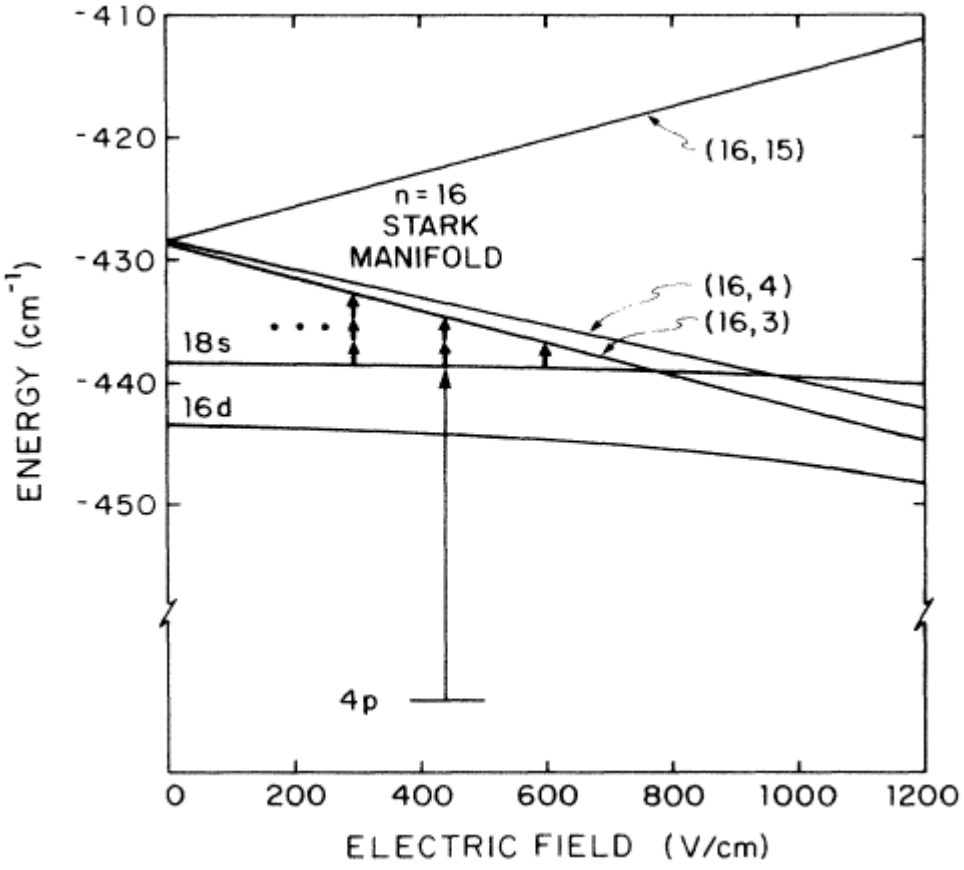

Excite atoms to the (n+2)s state with the laser in zero static field, add a microwave field, detect the n,3 Stark state

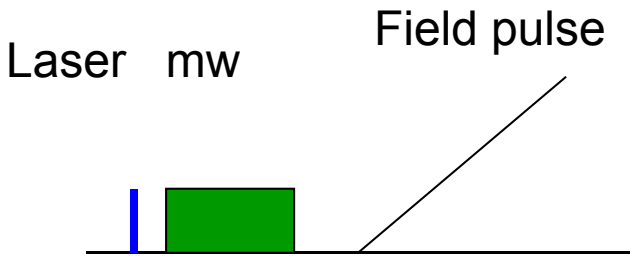

Sweep the microwave field amplitude over many shots of the laser, detect 16,3

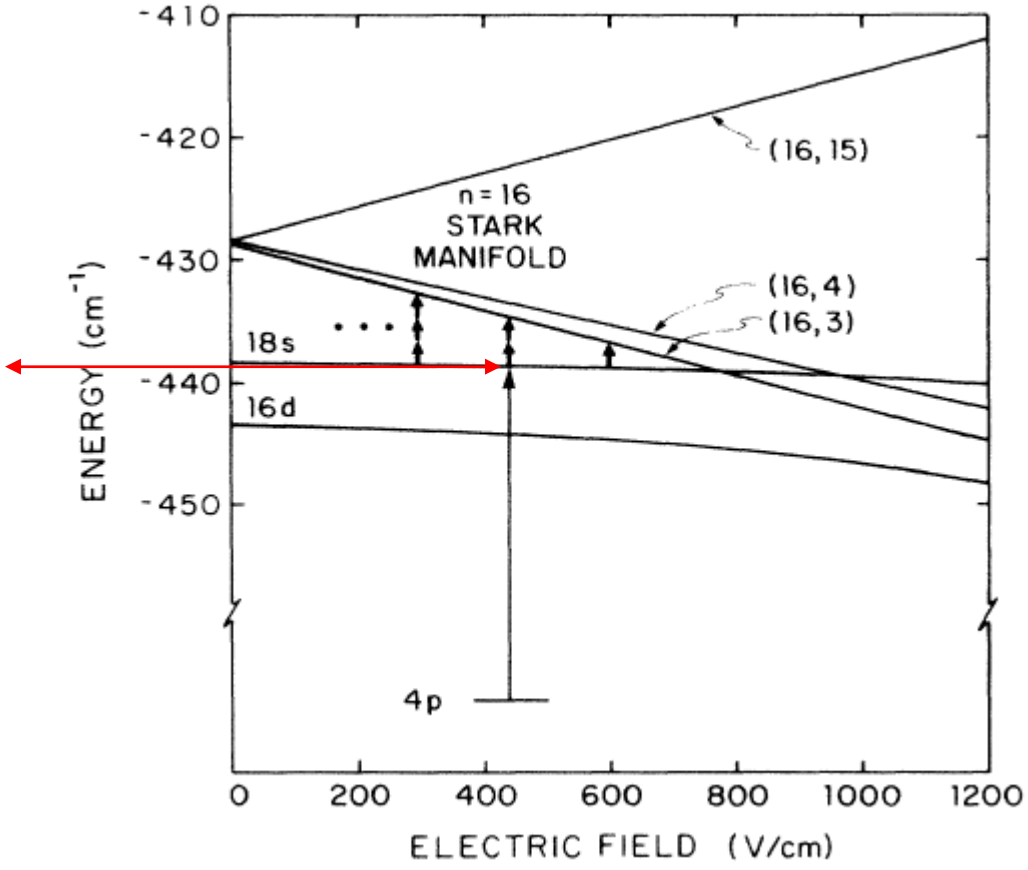

Excite 18s in zero static field, scan the amplitude of the 9.3 GHz microwave pulse,
And detect population in 16,3

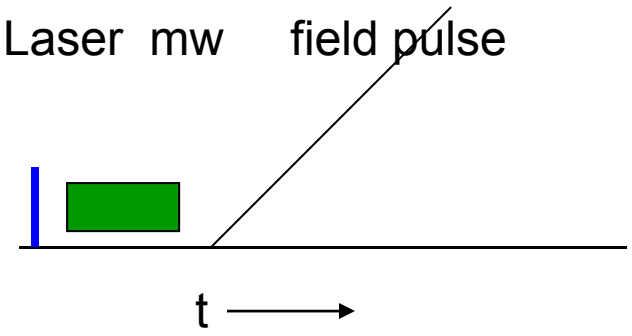

This is the expected result from microwave ionizaton; the microwave threshold is at the crossing field.

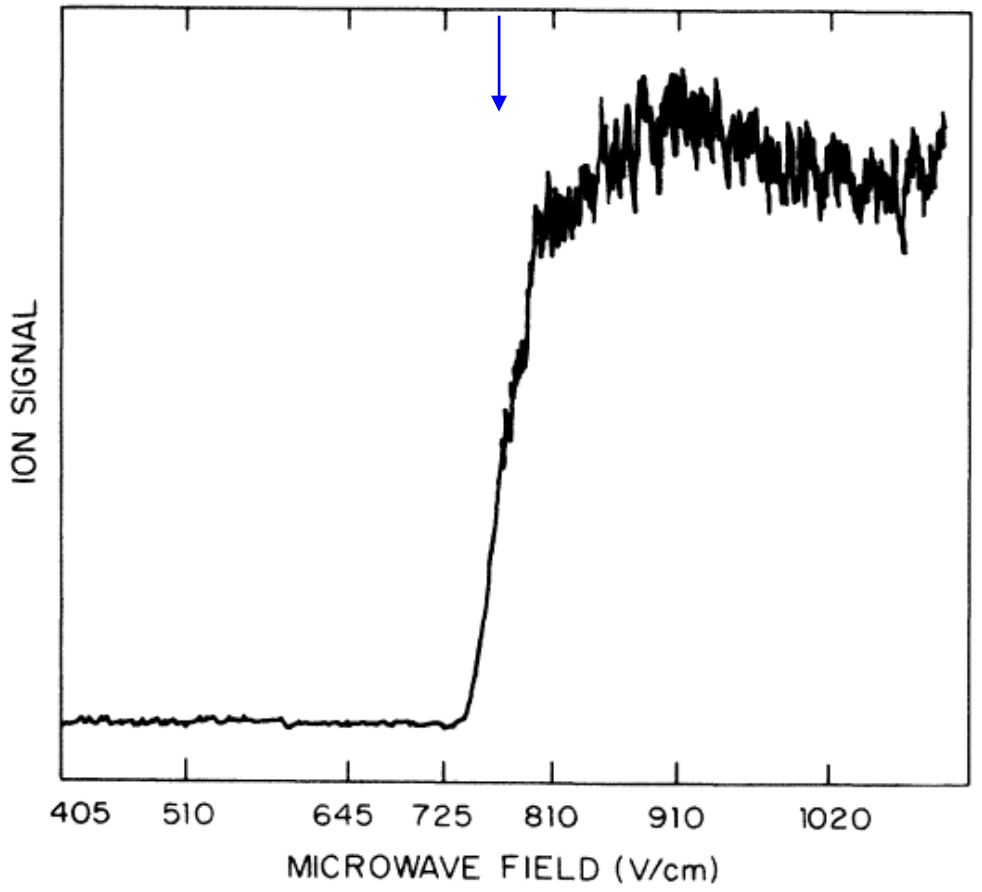

FIG. 3. Microwave threshold spectrum for transitions from the 18*s* state to the $n = 16$ Stark manifold.

Same experiment one state higher

What's this?

Multiphoton resonances
Power shifted into resonance

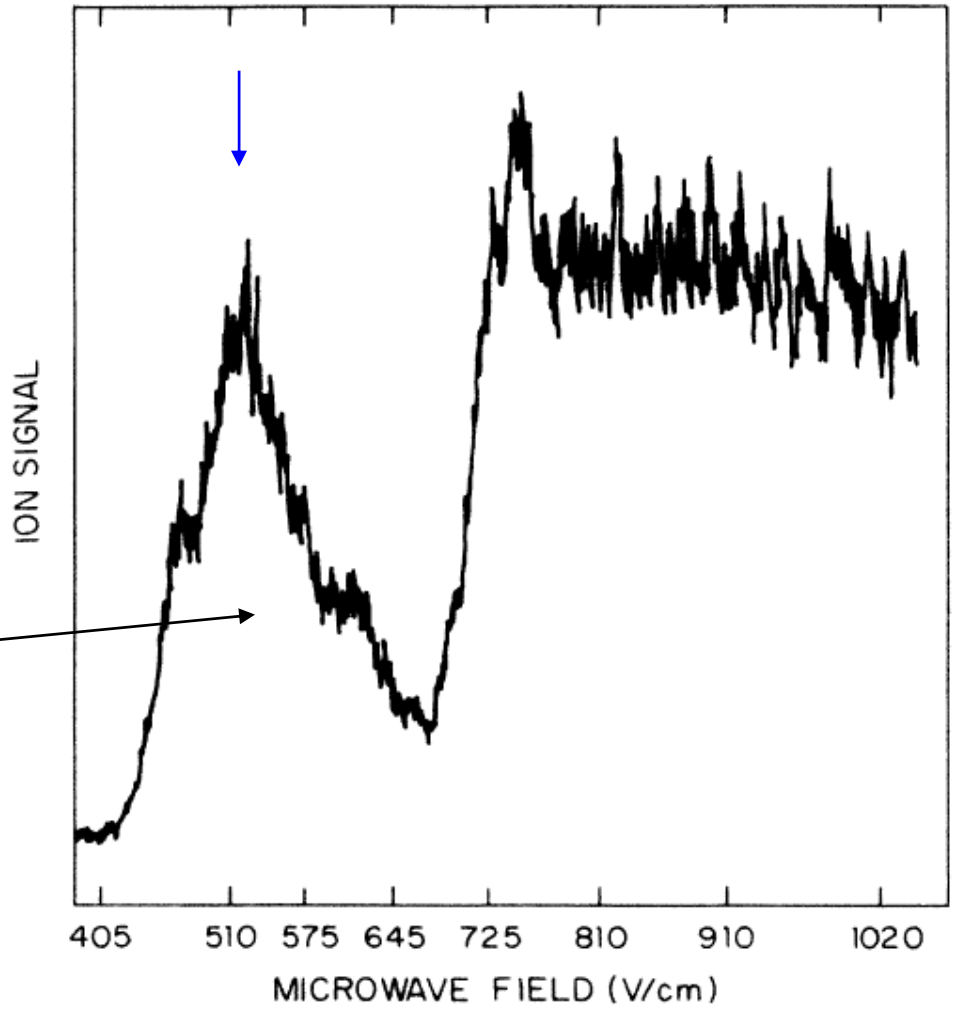

FIG. 4. Microwave threshold spectrum for transitions from the 19*s* state to the $n = 17$ Stark manifold. The resonance near 510 V/cm corresponds to the absorption of 27 microwave photons.

Now we fix the microwave field amplitude and scan the static field,
Laser excitation of (n+2)s, detection of n,3

Changing the static field changes the energy separation between the (n+2)s and n,3 Stark states.

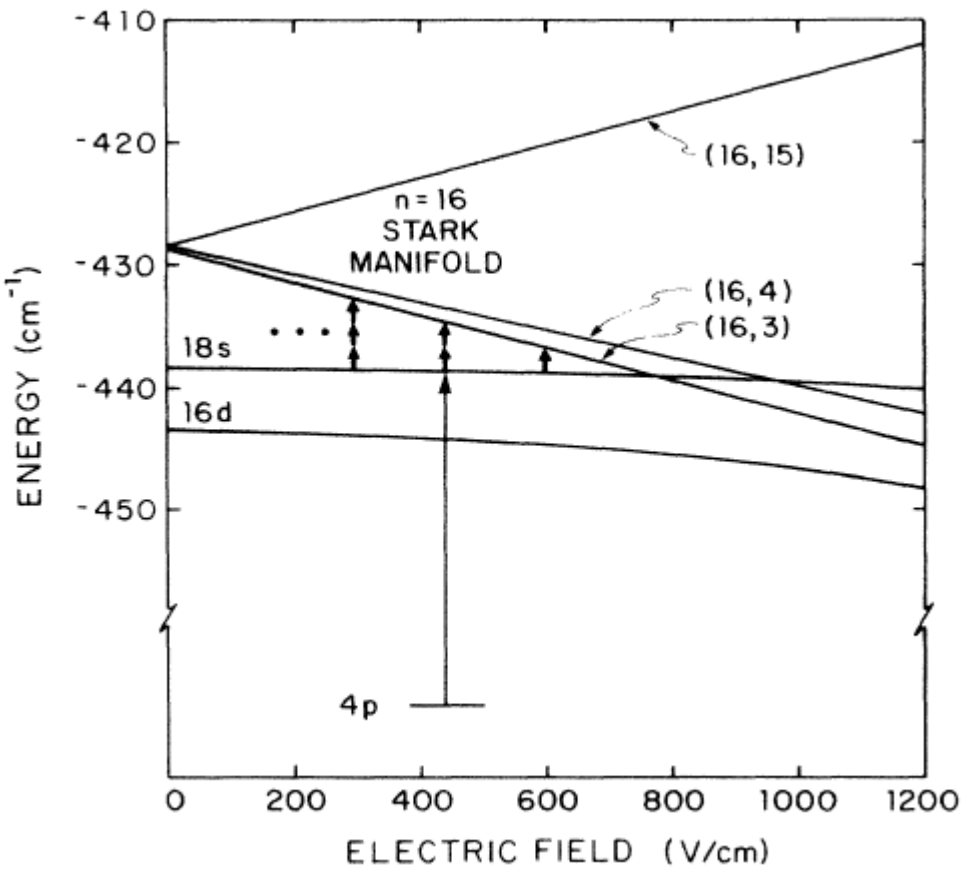

The K18s→16,3 transitions
At several microwave fields
Of frequency 10.5 GHz

Clear resonances for 1-28 photon transitions

‘Extra’ resonances
due to 16,k states, k> 3

Power shifts at high microwave fields

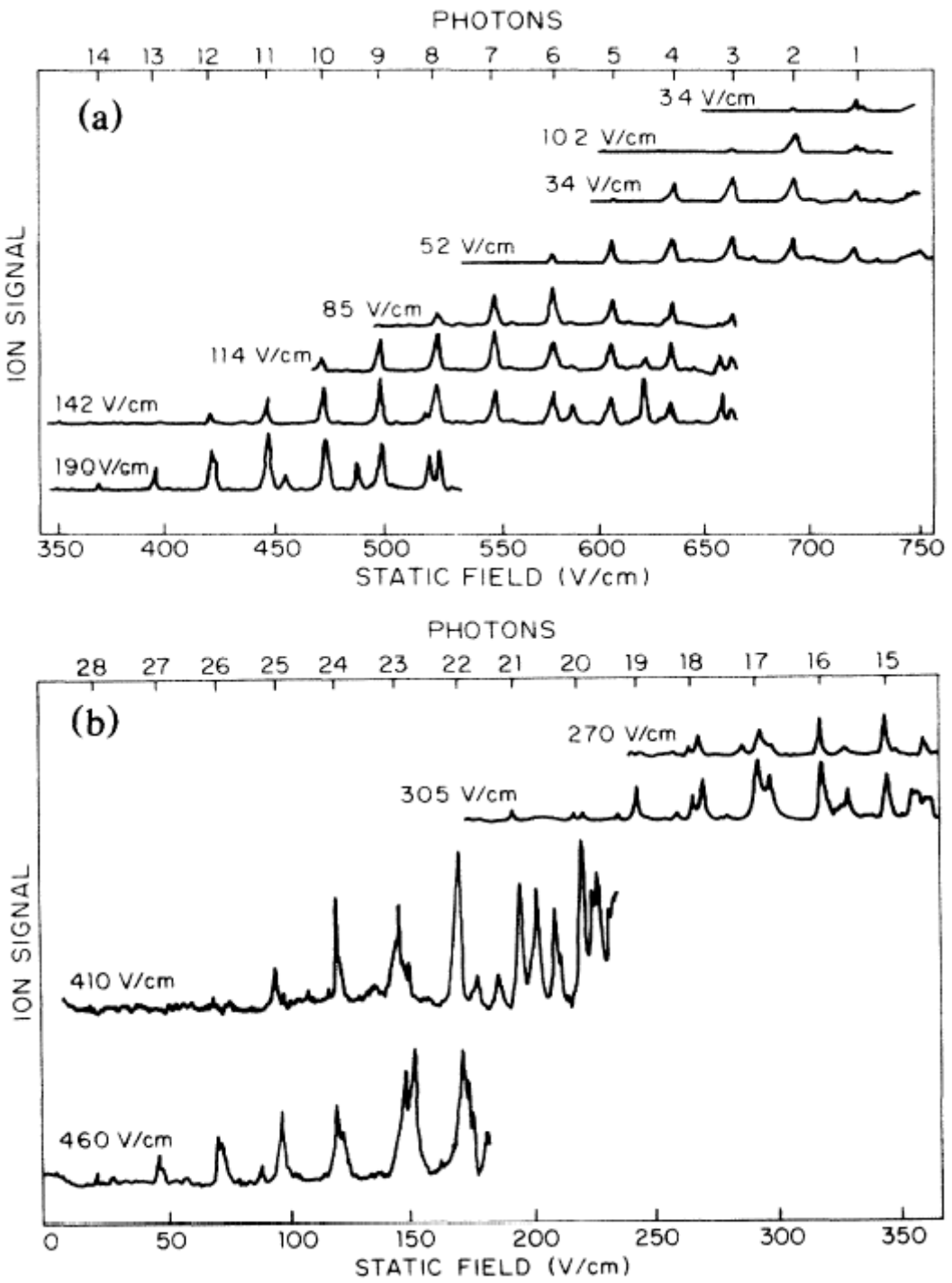

The number of photons absorbed increases linearly with the microwave field.

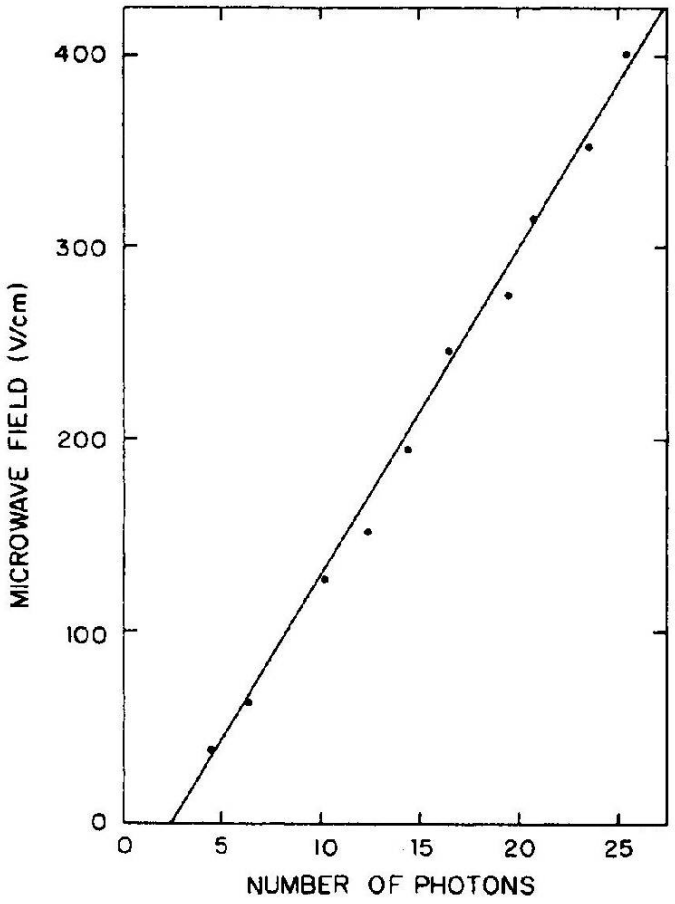

FIG. 6. Microwave field required to observe the 19*s*-to-(17,4) multiphoton transition vs the number of photons absorbed. The line is a least-squares fit to the data points, demonstrating that the total field, static plus microwave, required to drive the multiphoton transitions is constant. Note the two-photon offset at zero field.

How the Landau Zener, or time varying field picture leads to resonances

Two states 1&2, the wavefunction is

$$\psi = T_1(t)\left|1\right\rangle + T_2(t)\left|2\right\rangle$$

The core coupling producing the avoided crossing is

$$\left\langle 1\left|V_c\right|2\right\rangle = b$$

The Schrodinger equation leads to two coupled equations

$$i\dot{T}_1 = (W_1 - kF)T_1 + bT_2$$
$$i\dot{T}_2 = bT_1 + W_2T_2$$

where F is the instantaneous total field

$$F(t) = F_S + F_{MW}\cos\omega t$$

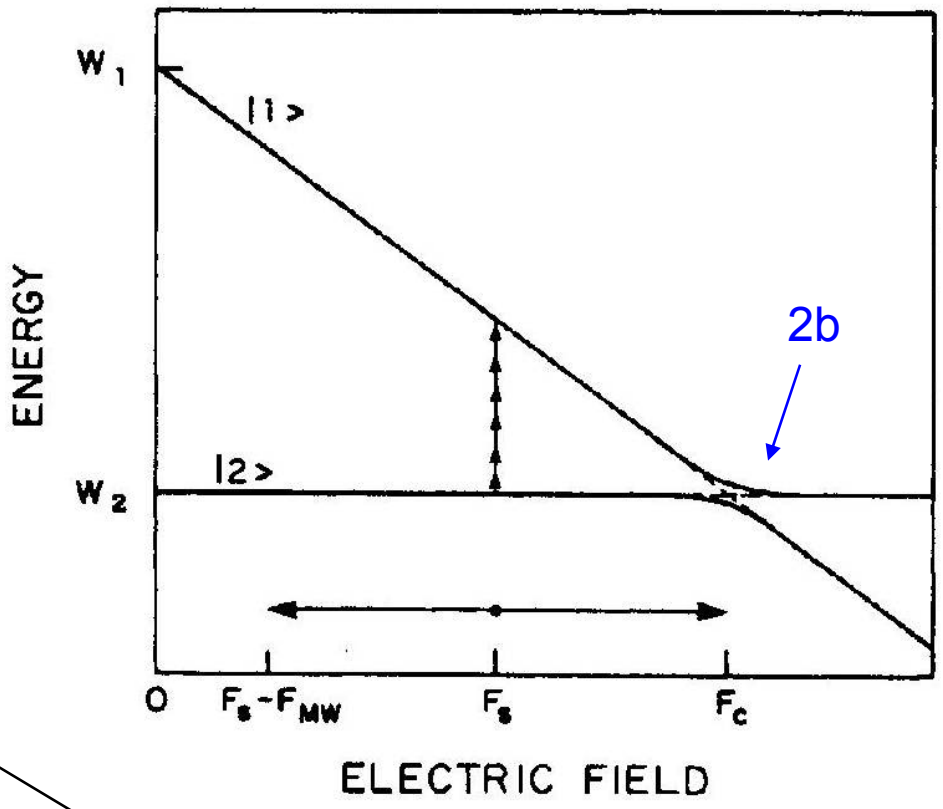

Solve by numerical integration over Many field cycles

In connecting field ionization to photionization the important parameter is the radiation frequency relative to the atomic frequency (scaled frequency). This is true for microwave and optical frequencies.

Many cycle Landau- Zener treatments connect field and photon points of view.

Collisions between Rydberg atoms

Resonant collisions

Resonant energy transfer is thought to be important in many contexts

He-Ne laser
CO_2 laser
photosynthesis

but there is no easy way to tune into or out of resonance.
There is no He-Ar laser.

Tuned Resonant Energy Transfer Collisions

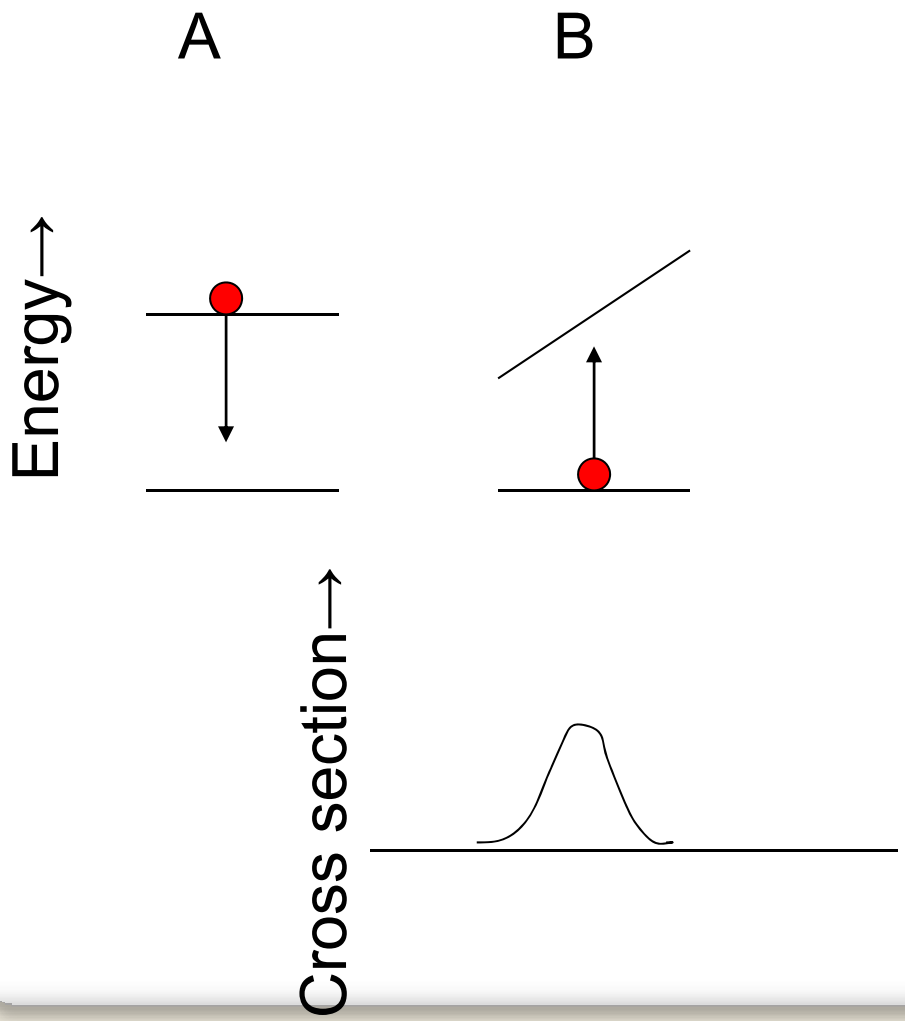

Resonant Dipole-dipole Collisions of two Na atoms

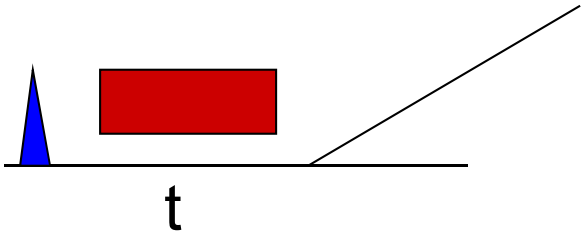

Populate 17s in an atomic beam

Collisions (fast atoms hit slow ones)

Field ramp to ionize 17p

Sweep field over many laser shots

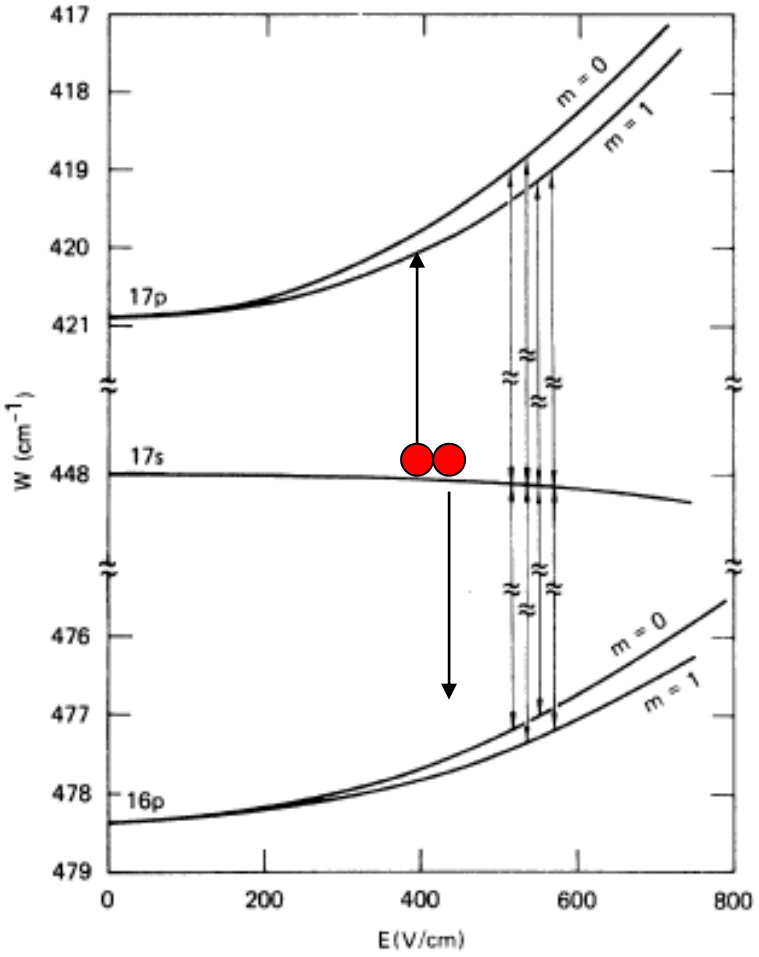

Safinya et al PRL 1980

Observed collisional resonances

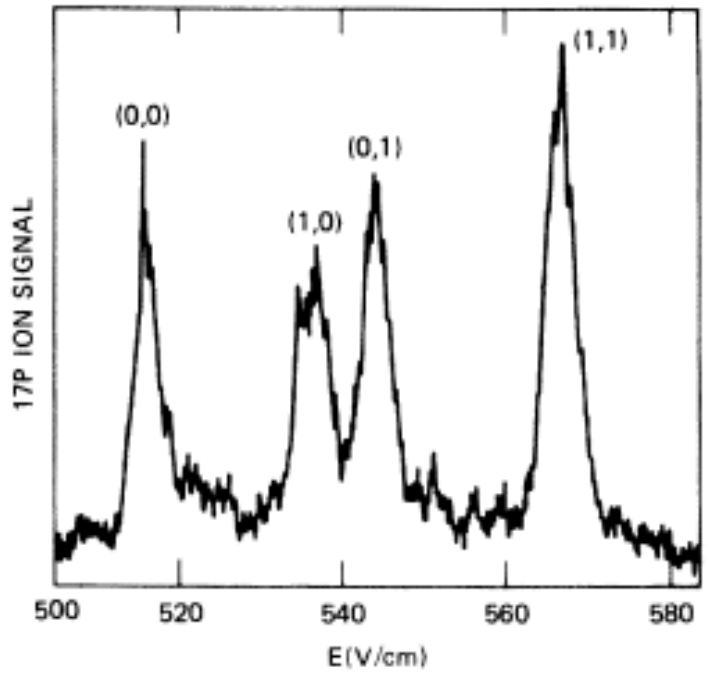

What is the cross Section?

What is the width?

Width: 1GHz

Collision rate=Nσv

$10^6 s^{-1} = 10^8 cm^{-3} \sigma 10^5 cm/s$

$\sigma = 10^{-7} cm^2 = 10^9 Å^2$

Gas kinetic cross section $100Å^2$ collision time 1ps

Dipole-dipole collision in terms of rf spectroscopy

Atom 1 has many oscillating Dipoles.

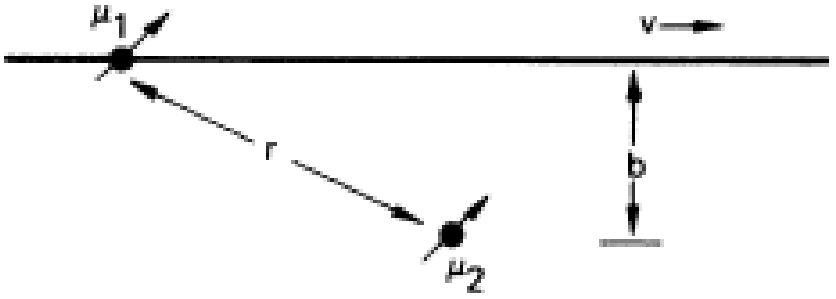

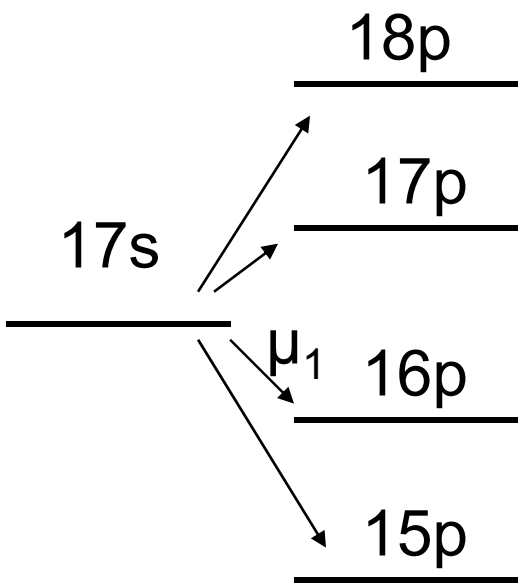

17s-16p dipole produces a field at Atom 2 of

$E_1=\mu_1/r^3 \cos\omega t$

Collision of atom 1 with atom 2

If E_1 drives the 17s-17p transition in Atom 2 the energy transfer occurs.

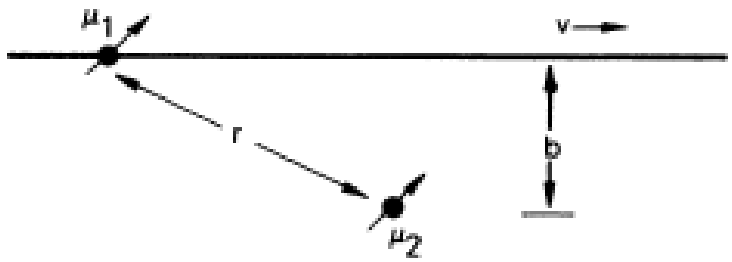

We require $\mu_2 E_1 t = 1$

$$\mu_2 \bullet \frac{\mu_1}{b^3} \bullet \frac{b}{v} = 1$$

$$b^2 = \frac{\mu_1 \mu_2}{v} \sim \frac{n^4}{v}$$

For n=20

Cross section $10^9\ a_0^2$ 10^{-7}cm^2

$$\frac{1}{t} = \frac{v}{b} = \frac{v^{3/2}}{n^2}$$

Width $0.2\text{x}10^{-8}$ 1GHz

Measurement of the cross section

Measure the fractional population
Transfer as a function of the time
and the density

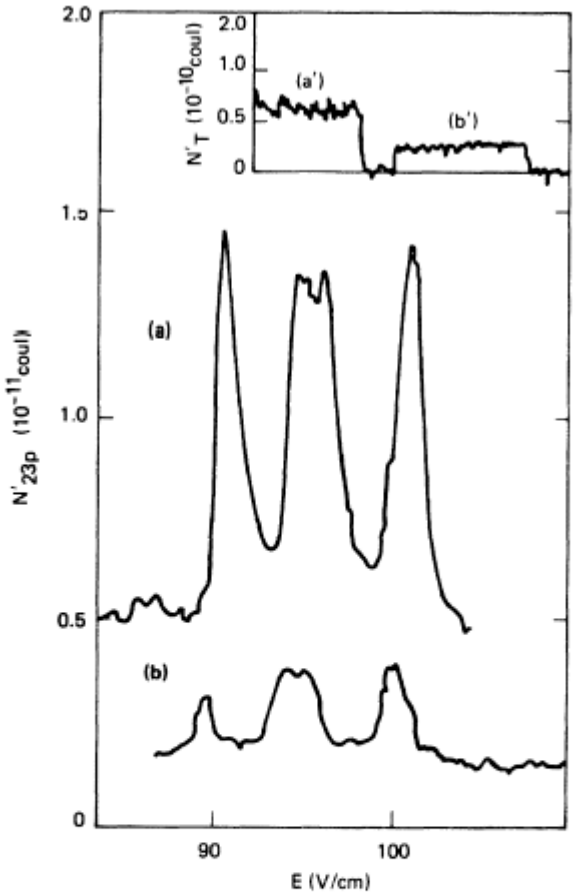

FIG. 8. (a) The population of the 23*p* state 2 μsec after the population of the 23*s* state showing the collisional resonances. Notice that the (0,1) and (1,0) resonances are not resolved in this trace. (b) The same as (a) except with 40% of the blue-laser power. (a′) A recording of the total populations in the 23*s*, 22*p*, and 23*p* states taken simultaneously with (a). (b′) A recording of the total populations in the 23*s*, 22*p*, and 23*p* states taken simultaneously with (b).

Observed values of the cross sections and widths

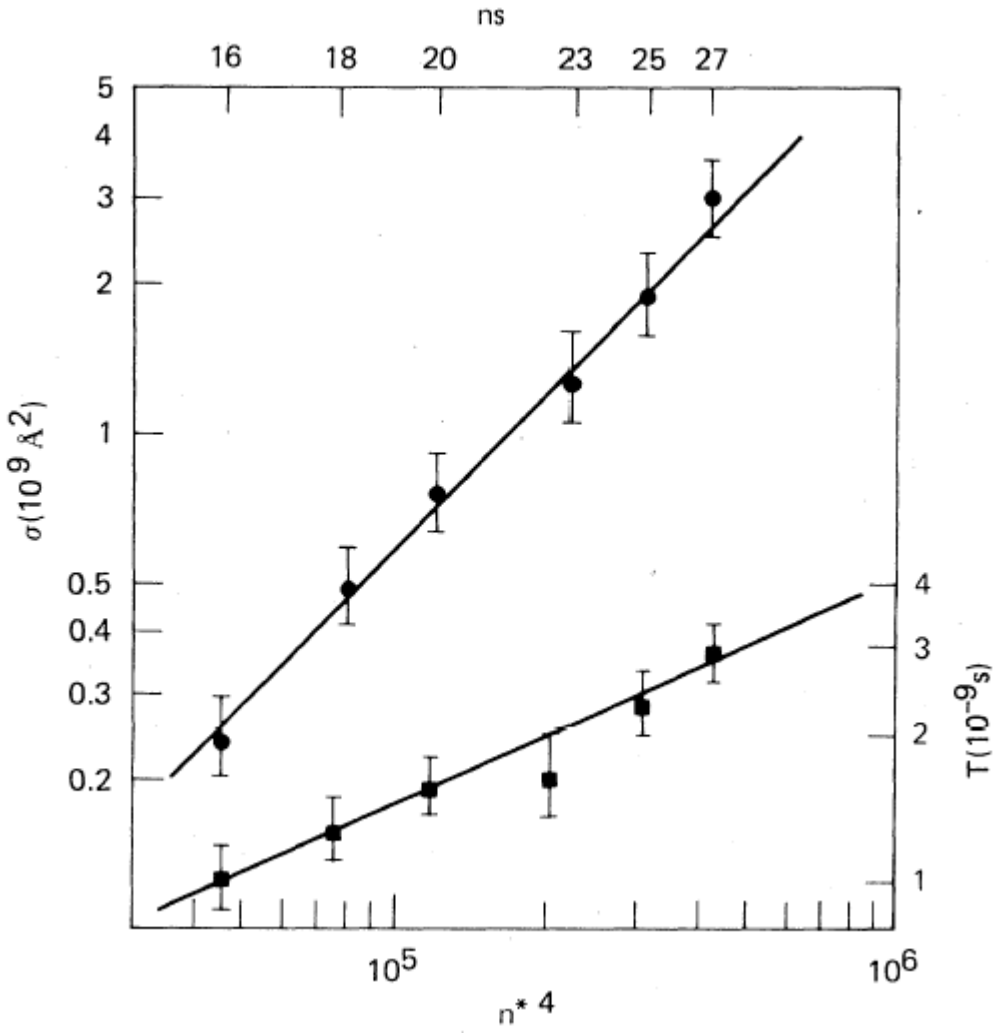

Calculating the collision cross section

We calculate the transition probability for impact parameter b and velocity v.

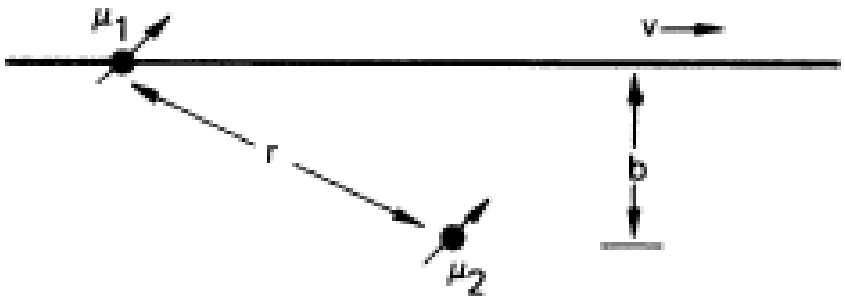

Initial state: two ns (s) atoms, final state one np (p) and one (n+1)p (p')

$$V = \frac{\bar{\mu}_1 \cdot \bar{\mu}_2}{r^3} - \frac{3(\bar{\mu}_1 \cdot \bar{r})(\bar{\mu}_2 \cdot \bar{r})}{r^5}$$

Consider two states ss and pp'

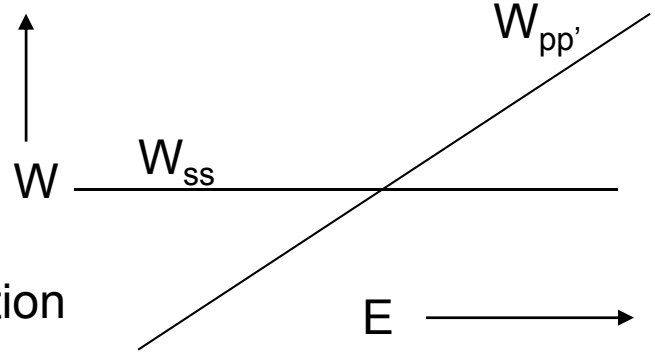

$$\psi_{ss} = \psi_{1s} \otimes \psi_{2s}$$

$$\psi_{pp'} = \left(\psi_{1p} \otimes \psi_{2p'} + \psi_{1p'} \otimes \psi_{2p}\right)/\sqrt{2}$$

They are coupled by the dipole dipole interaction matrix elements

$$V_{ss,pp'} \quad \text{and} \quad V_{pp',ss}$$

The time dependent wavefunction is given by

$$\psi(t) = C_{ss}(t)\psi_{ss} + C_{pp'}(t)\psi_{pp'}$$

Putting this wavefunction into the Schrodinger equation gives the two equations

$$i\dot{C}_{ss} = V_{pp',ss}C_{pp'}$$

I have assumed that W_{ss} =0

$$i\dot{C}_{pp'} = W_{pp'}C_{pp'} + V_{ss,pp'}C_{ss}$$

These equations are easily solved by a computer, and may be solved analytically In several cases. One is the “box interaction,” assuming the interaction to be present during –b/v<t<b/v. This gives the width of the resonance and the peak cross section.

Assuming that the system was in the ss state at t=-∞, and that the two states are in resonance, $W_{pp'}$ =0, the solutions at time t are

$$C_{ss}(t) = \cos\left(\int_{-\infty}^{t} V_{ss,pp'} dt' \right)$$

$$C_{pp'}(t) = \sin\left(\int_{-\infty}^{t} V_{pp',ss} dt' \right)$$

The transition probability from ss to pp’ is $C_{pp'}^{2}(\infty)$

Note that it is a function of b!

We need to write the explicit form of the interaction matrix element.

There are two natural axes, the field, which specifies the direction of the dipoles, and the velocity.

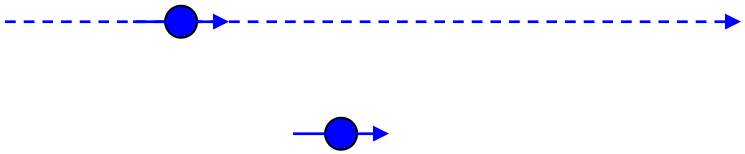

v parallel to E

v perpendicular to E

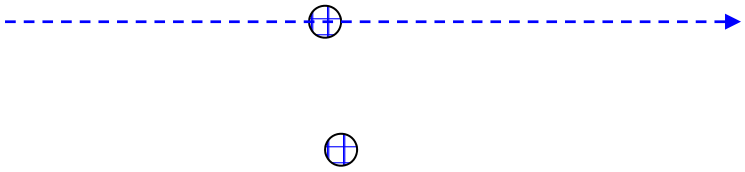

dipoles in the plane perpendicular to v

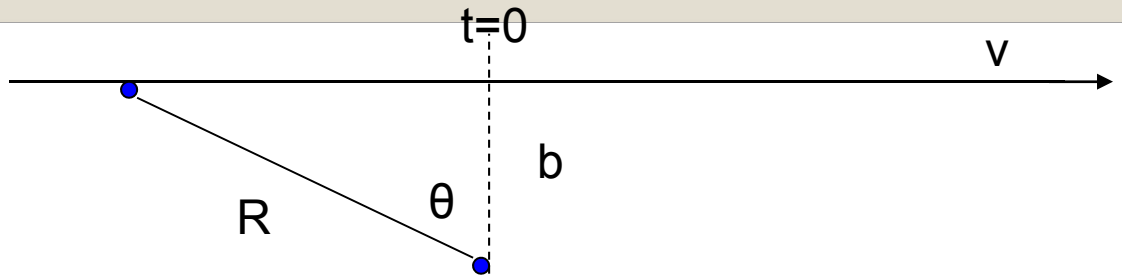

v parallel to E

$$V_{ss,pp'} = \frac{\mu_z \mu_z' \left(1 - 3\sin^2\theta\right)\cos^3\theta}{b^3}$$

v perpendicular to E

In addition to θ, we define φ as the angle between the field, the z direction, and the plane of the page. In this case

$$V_{ss,pp'} = \frac{\mu_z \mu_z' \left(1 - 3\cos^2\theta \sin^2\varphi\right)\cos^3\theta}{b^3}$$

During a collision φ is constant and θ varies from –π/2 to π/2. To compare to an experiment requires averaging over φ.

Using the appropriate V we calculate $C_{pp'}(\infty)$ for a fixed b. Since it is a function of b we write it explicitly as such.

$$C_{pp'}(b,\infty) = \sin\left(\int_{-\infty}^{t} V_{pp',ss}\, dt' \right)$$

The cross section is given by

$$\sigma = \int_{0}^{\infty} 2\pi b C_{pp'}^{2}(b,\infty)\, db$$

The integral has the following form

$$\int_{-\infty}^{\infty} V_{ss,pp'}\, dt = \frac{\mu\mu'}{vb^{2}} G$$

Where G is a geometrical factor of order unity.

If we define b_0 such that

$$\frac{\mu\mu'}{vb_0^2}G = \frac{\pi}{2}$$

Then for $b<b_0$ the sin function oscillates, and a reasonable approximation to the cross section is

$$\sigma = \pi b_0^2$$

Which is proportional to the dipole dipole coupling.

An interesting aspect of the v parallel to E collision is that, integrated over the collision, the interaction vanishes.

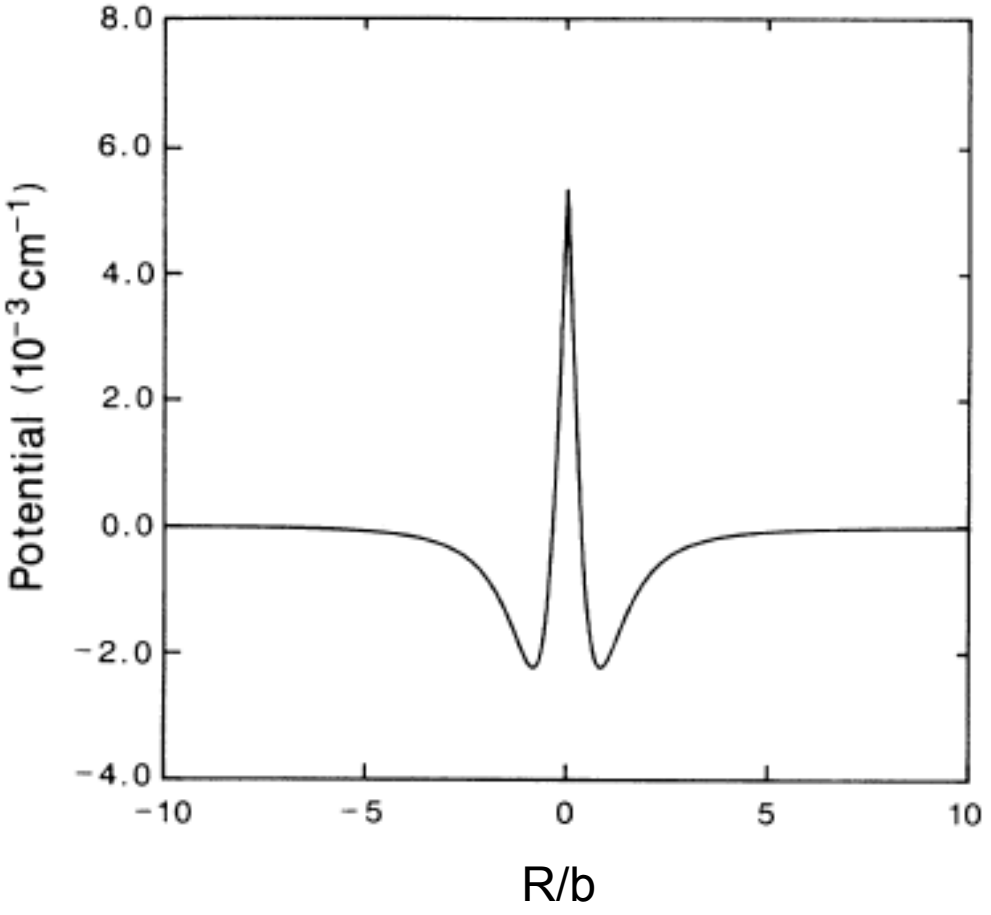

Observing the difference between v and E parallel and perpendicular

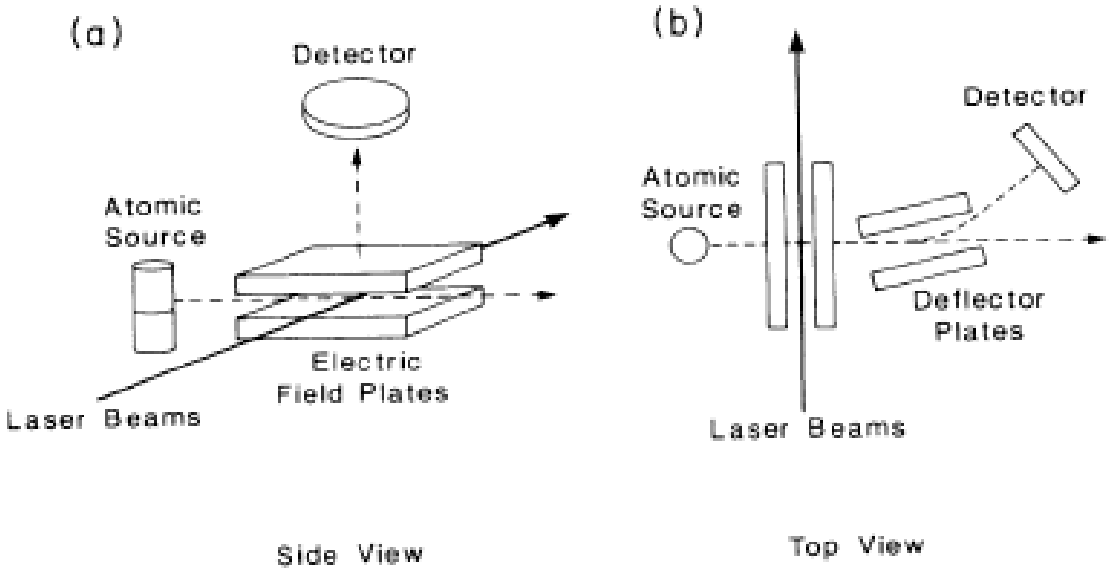

FIG. 7. Experimental apparatus configured so that (a) the electric field is perpendicular to the collisional velocity, and (b) the electric field and collisional velocity are parallel.

v parallel to E

v perpendicular to E

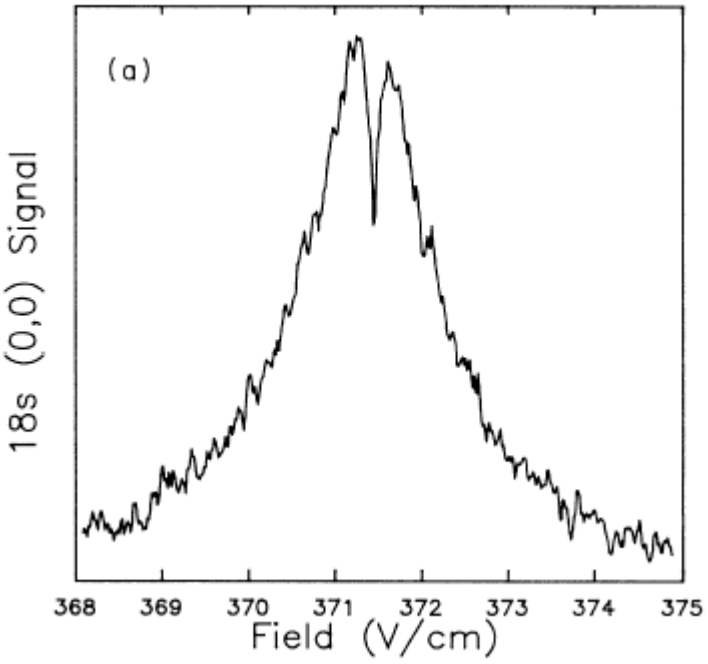

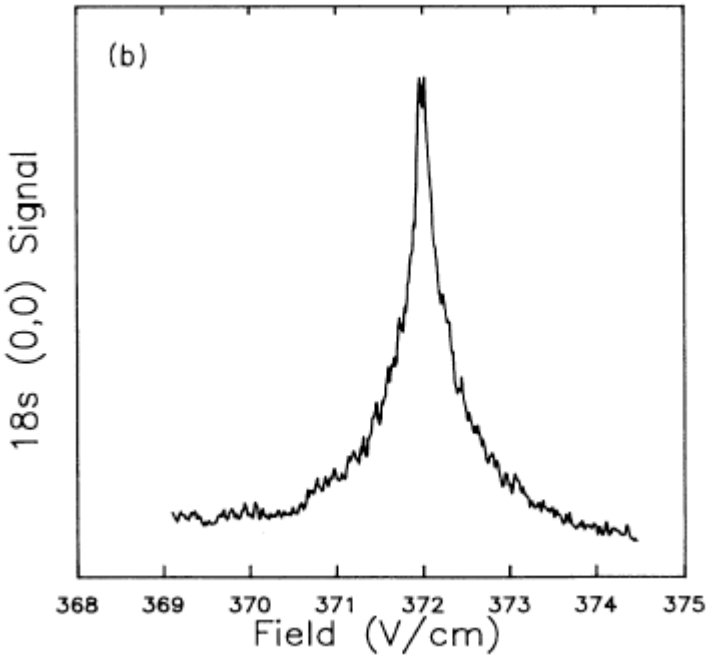

dip in the center, broader resonance

narrow resonance

The velocity dependence of collisions of K atoms

$$\sigma = \frac{\mu\mu'}{v} \qquad \frac{1}{t} = \sqrt{\frac{\mu\mu'}{v^3}}$$

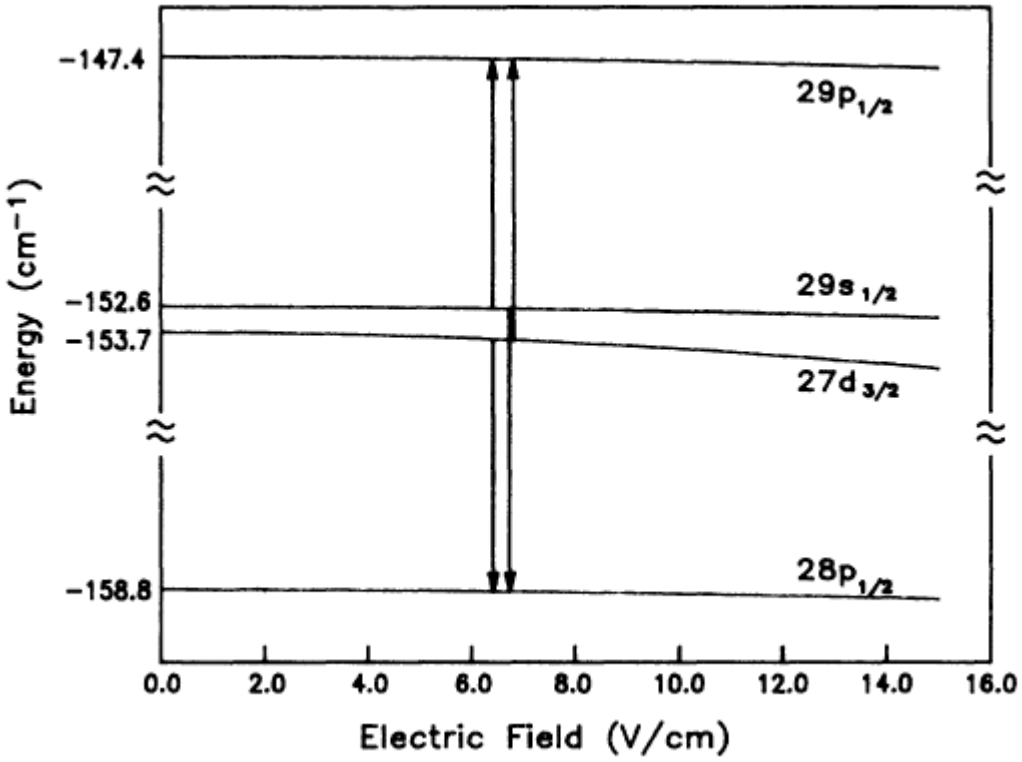

Stoneman et al PRL

Experimental Approach

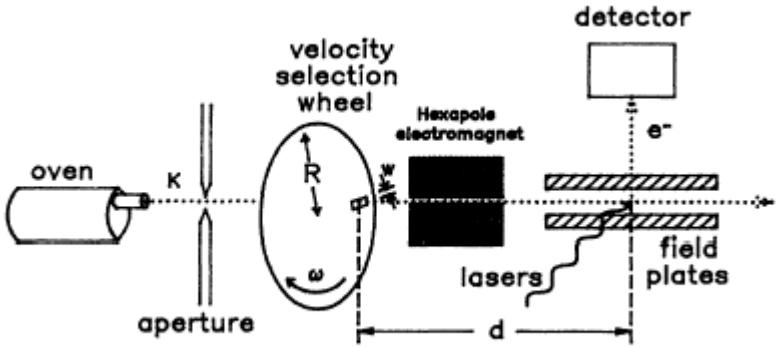

FIG. 1. Experimental apparatus.

L N_2 trap

cell

beam

velocity
Selected
Beam T=1K

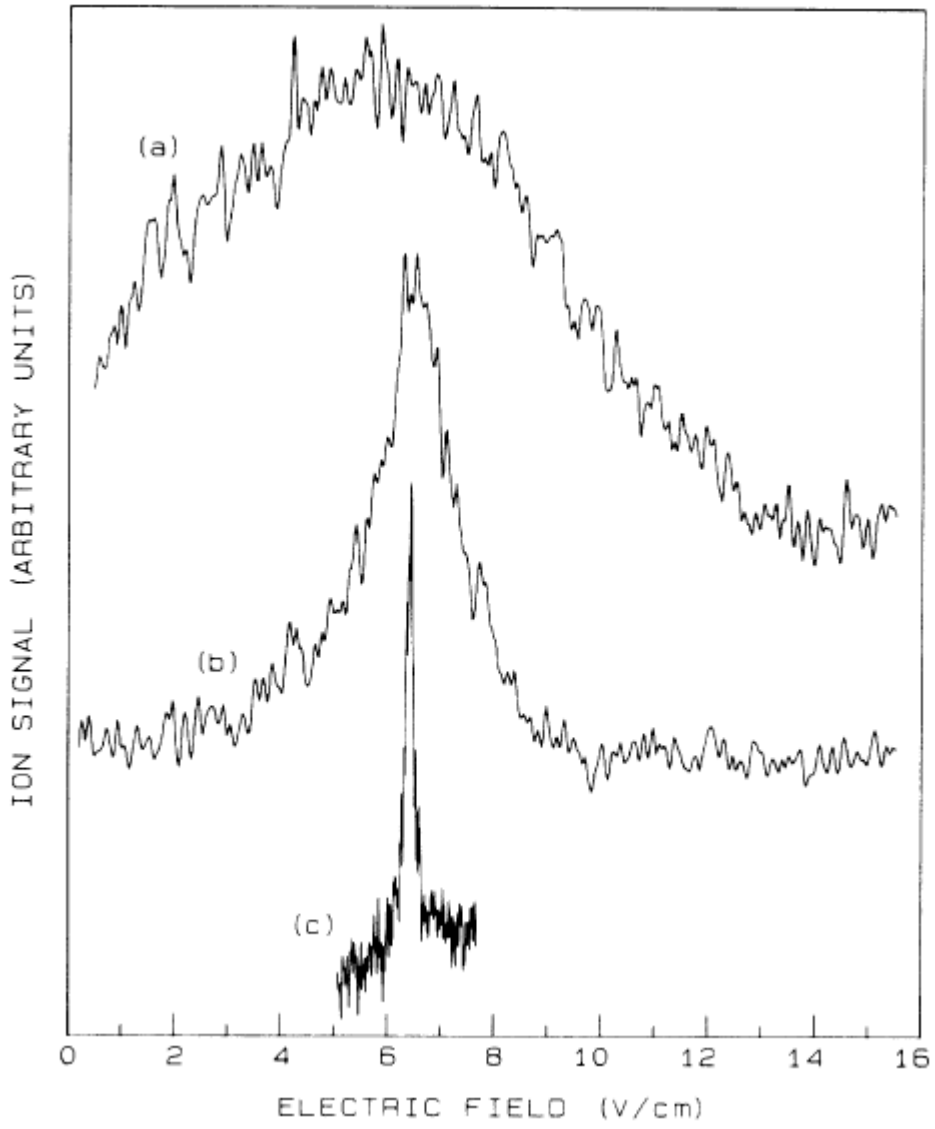

240 MHz

57 MHz

6 MHz

Resonant dipole-dipole collisions of Rydberg atoms ave enormous cross sections and long durations, and they are easy to understand.

They are a good test bed.

Collisions between Rydberg atoms

Radiatively assisted collisions

Radiatively Assisted Collisions

Dipole –dipole interactions in the frozen Rydberg gas

Radiatively assisted collisions

While excited atom A collides with ground state atom B, making a transient molecule, they absorb a photon,producing a ground state atom A and an excited atom B.

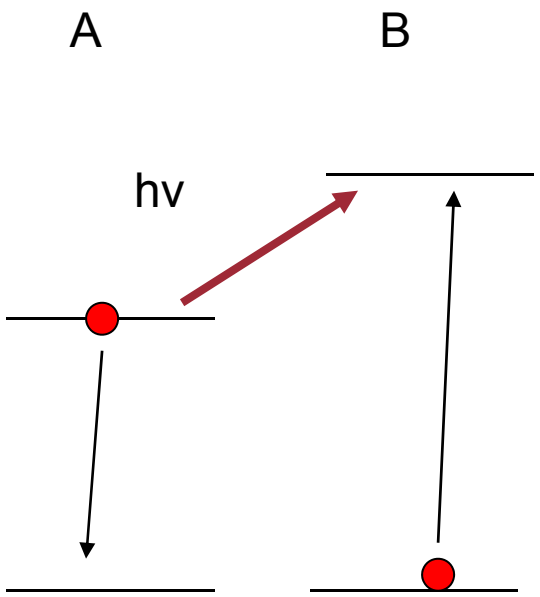

The collision lasts 1ps, and the dipole moments are $1ea_0$.

Rabi frequencies of 10^{12} Hz are required. With dipoles of 1 ea_0 fields of 1 MV/cm are required.

These are hard to observe.

$$\mu E t = 1$$

$$\mu E = 1/t$$

The Rydberg alternative

Whle excited atom A collides with ground state atom B, making a transient Molecule, they absorb a photon,producing a ground state atom A and an excited atom B.

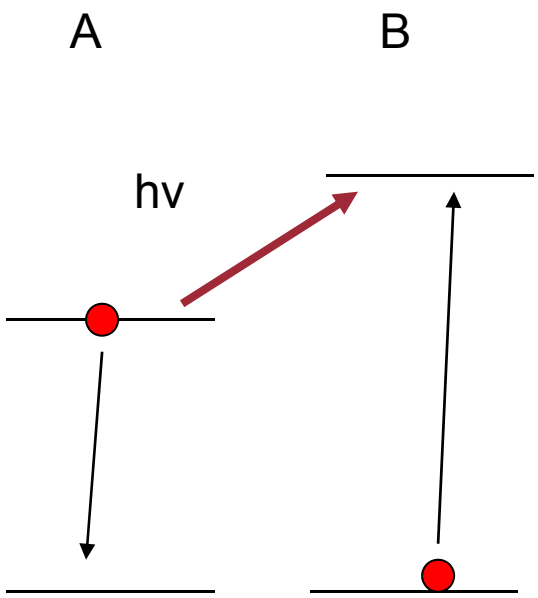

The collision can last 10 ns, and the dipole moments are $400ea_0$.

Now Rabi frequencies of 10^8 Hz are required. With dipoles of 400 ea_0 Fields of 0.25 V/cm are required.

The field requirement is reduced by 10^6, and the power by 10^{12}. Multi-Photon processes should be visible.

The Rydberg alternative

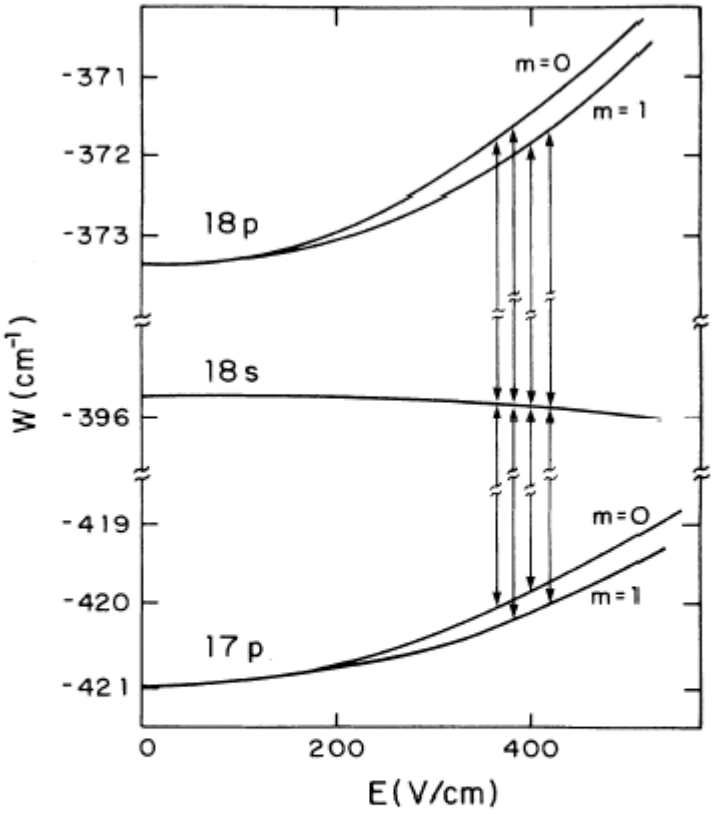

FIG. 3. Energy-level diagram for 17*p*, 18*s*, 18*p* states in a static electric field. The vertical lines are drawn at the four fields where the *s* state is midway between the two *p* states and the resonance collisional transfer occurs. Similar sets of four lines would be drawn for each multiphoton-assisted radiative collision process.

The microwave assisted collisions

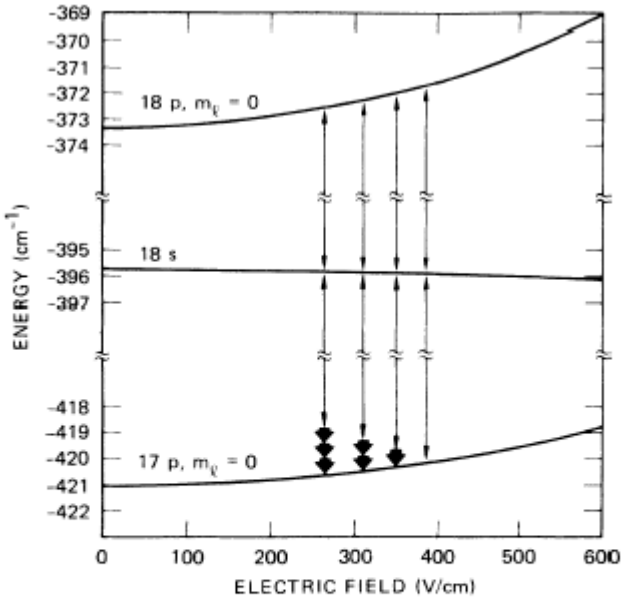

FIG. 2. Stark energy-level diagram of the $|m_l| = 0$ states, relevant to the multiphoton-assisted collisions. The vertical lines indicate the collisional transfer and are drawn at the fields where they occur. The thick arrows correspond to the emitted or absorbed photons.

The apparatus

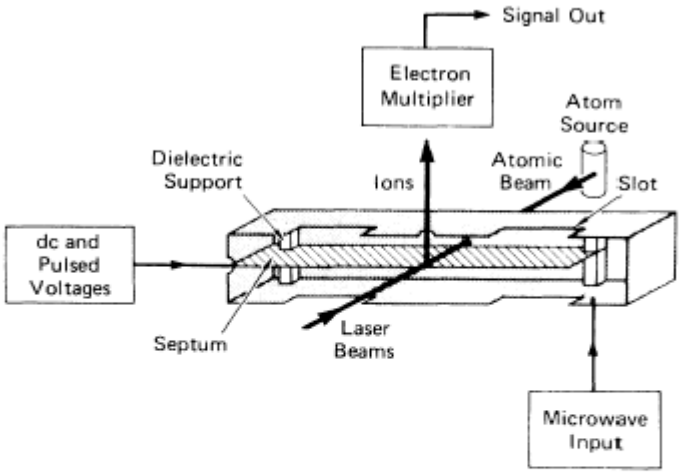

FIG. 5. Main features of the atomic-beam apparatus, the atomic source, the microwave cavity, and the electron multiplier. The microwave cavity is shown sliced in half. The copper septum bisects the height of the cavity. Two holes of diameter 1.3 mm are drilled in the side walls to admit the collinear laser and Na atomic beams, and a 1-mm hole in the top of the cavity allows Na^+ resulting from field ionization of Na to be extracted. Note the slots for pumping.

Pillet et al

Observed radiatively assisted collisions

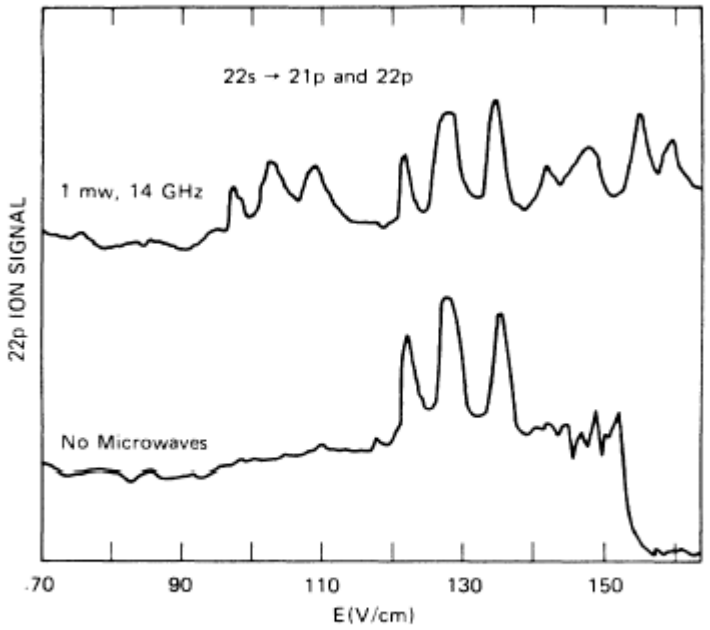

FIG. 6. Observed 22*p*-ion signal after the population of the 22*s* level, with and without 1 mW of 14 GHz microwave power.

The cavity Q is 1200, so the effective power is 1.2W

The Na 18s+18s→mhv +17p+18p resonances
In different 15.5 GHz microwave fields

0 V/cm

13.5 V/cm

50 V/cm

105 V/cm

165 V/cm

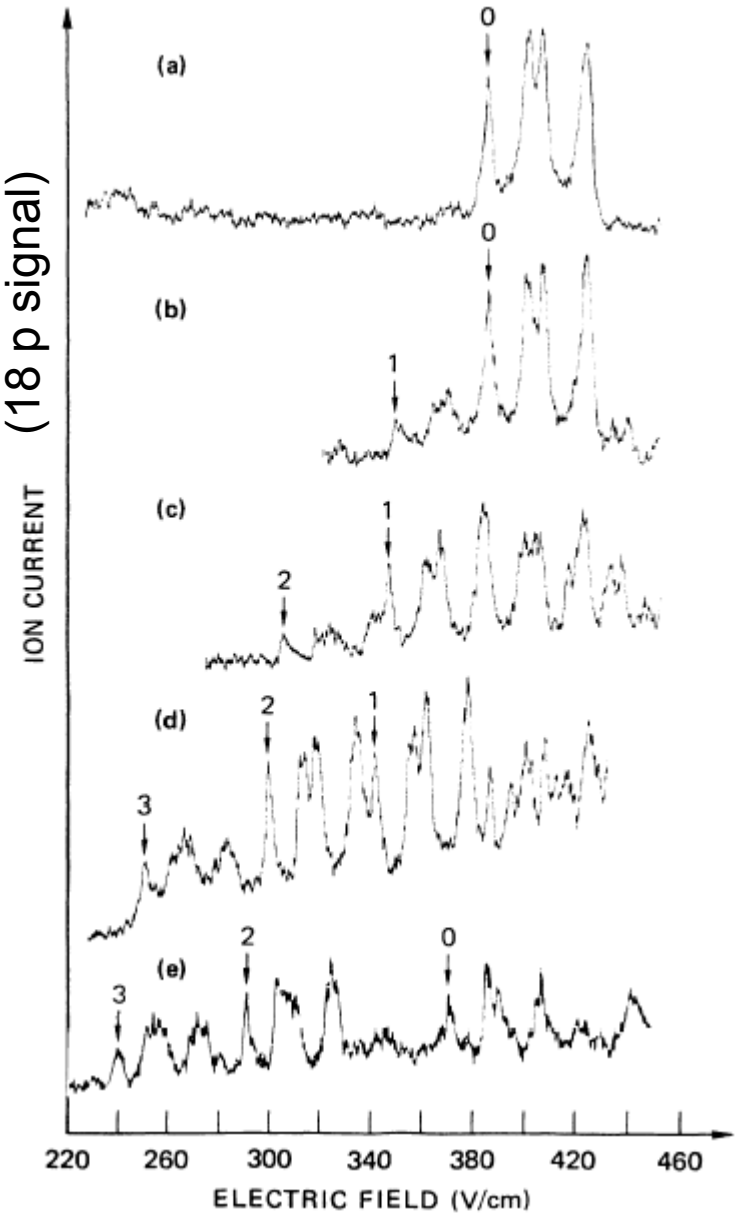

Plots of the signals (relative cross sections) vs 15.5 GHz microwave power for the m photon resonances

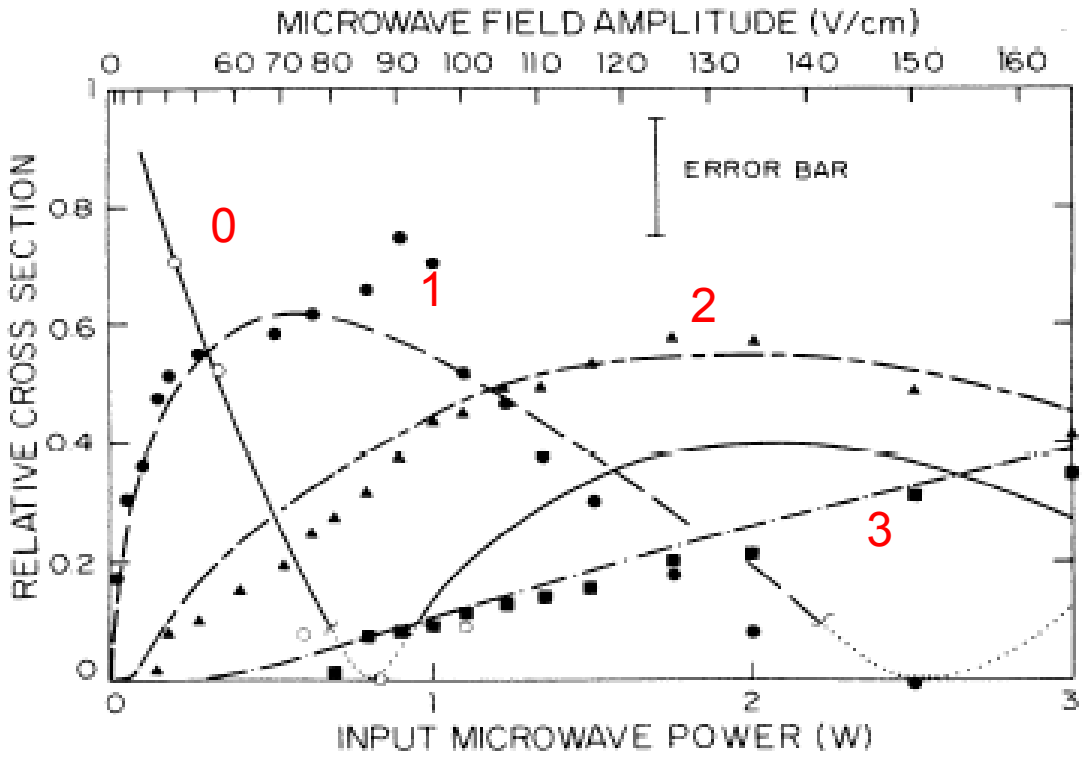

Theoretical description

We first recall how we calculated the resonant collision cross sections.

Since multiple microwave photons are absorbed or emitted,
we consider the effect of the field on the atoms, making dressed states

We then calculate the cross sections using the dressed states.

In the treatment of resonant collisions we introduced the direct product states ss and pp'

$$\psi_{ss} = \psi_{1s} \otimes \psi_{2s}$$

$$\psi_{pp'} = \left(\psi_{1p} \otimes \psi_{2p'} + \psi_{1p'} \otimes \psi_{2p}\right)/\sqrt{2}$$

They are coupled by the dipole dipole interaction matrix elements

$$V_{ss,pp'} \text{ and } V_{pp',ss}$$

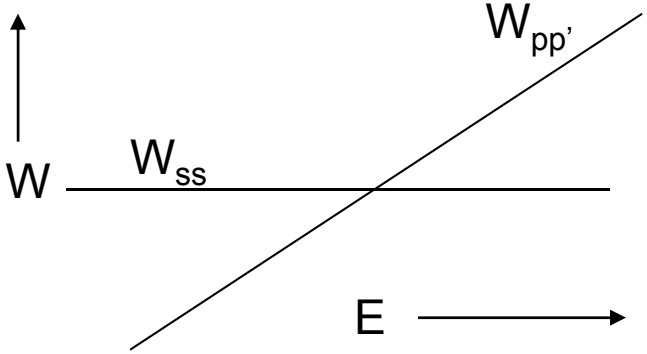

At R=∞ the levels cross at the resonance field.

At any finite R the levels have an avoided crossing of size 2V, due to the dipole-dipole interaction V.

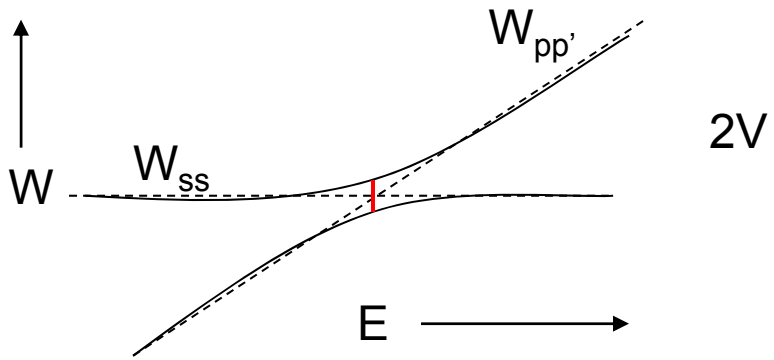

The transition probability for a trajectory with impact parameter b is

$$C^2_{pp'}(b,\infty) = \sin^2\left(\int_{-\infty}^{\infty} V_{pp',ss}\,dt'\right)$$

The cross section is determined by the impact parameter b_0 for which the integral has the value π/2. Since

$$\sigma \propto b_0^2 \propto V = \frac{\mu\mu'}{R^3}$$

the cross section is proportional to the avoided crossing at any R.

Now we consider the MW field.

In an electric field near the resonance field the energies of the ss and pp' states are given by

$$W_{ss} = W_{s0}$$

$$W_{pp'} = W_{p0} + k(E(t) - E_0)$$

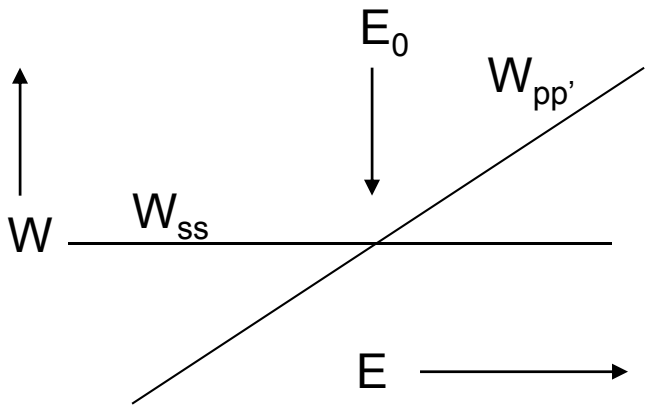

Here k is the sum of the Stark coefficients of the p and p' states.

The total field is $E(t) = E_S + E_{MW} \cos \omega t$

And the instantaneous energy of the pp' state is

$$\tilde{W}_{pp'}(t) = W_{p0} - k(E_S - E_0) - kE_{MW} \cos \omega t$$

The microwave field modulates the energy of the pp' state. This the same problem we saw before.

In the absence of any coupling to the ss state the pp' state would be given by

$$C_{pp'}(t)\psi_{pp'}$$

where

$$C_{pp'}(t) = e^{-i\int_{t_0}^{t}\left(W_{p0}+k(E_S-E_0)+kE_{MW}\cos\omega t'\right)dt'}$$

$$C_{pp'}(t) = e^{-i\left(W_{p0}+k(E_S-E_0)\right)t}\cdot e^{-i\frac{kE_{MW}}{\omega}\sin\omega t}$$

Which we can expand as a Bessel function expansion

$$C_{pp'}(t) = e^{-i\left(W_{pp'}+k(E_S-E_0)\right)t}\cdot\sum J_m\left(\frac{kE_{MW}}{\omega}\right)e^{-im\omega t}$$

Finally,

$$\psi_{pp'} C_{pp'}(t) = \psi_{pp'} e^{-i(W_1 - kE_S)t} \cdot \sum J_m \left(\frac{kE_{MW}}{\omega} \right) e^{-im\omega t}$$

The original pp' state has been replaced by a carrier and sideband states

The sidebands have appreciable amplitude for $m = kE_{MW} / \omega$

Or the energy span is $m\omega = kE_{MW}$

In terms of the energy level picture

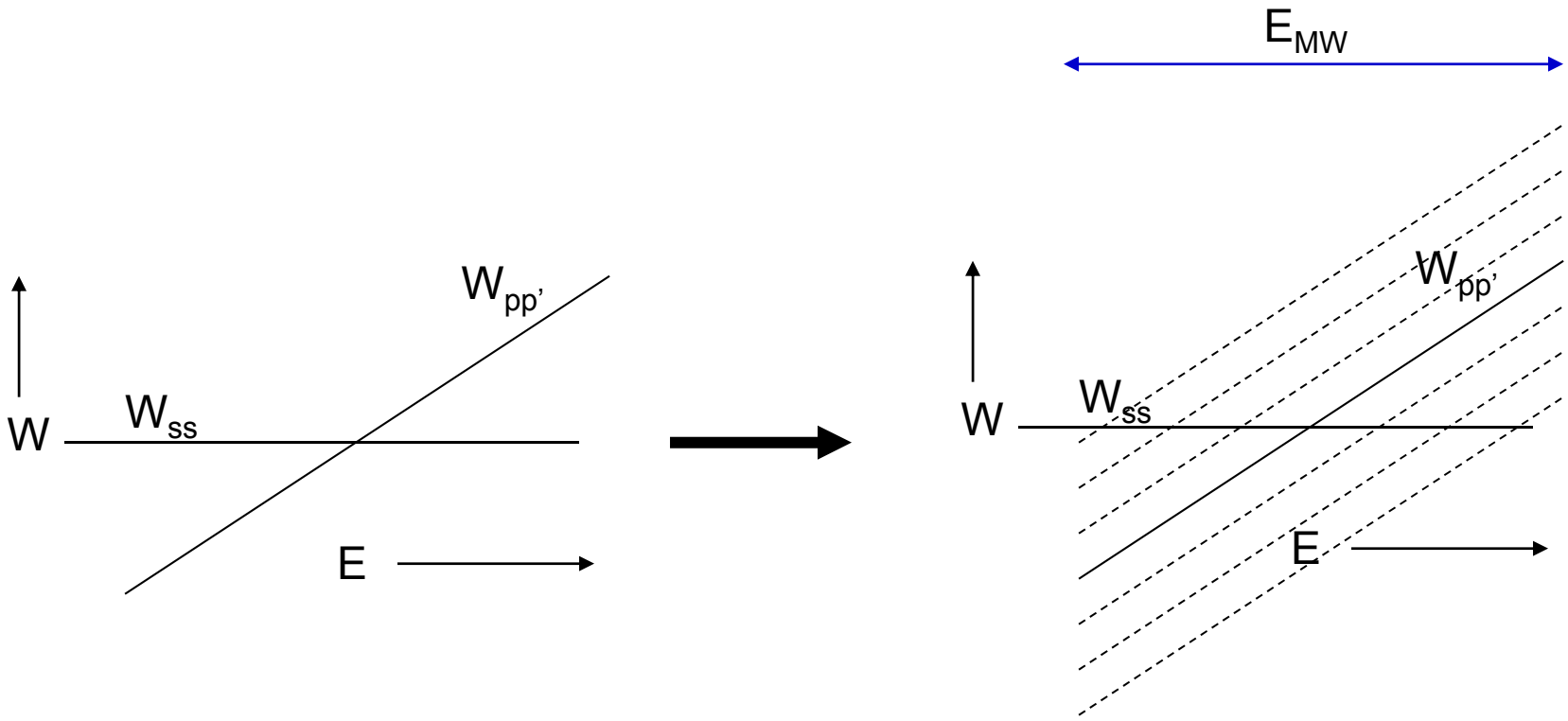

Each of the pp' sideband states crosses the ss state,
and has an avoided crossing at finite R.

The dipole dipole coupling between the mth sideband state and the ss state is

$$V_{ss,pp'm} = V_{ss,pp'} J_m\left(\frac{kE_{MW}}{\omega}\right)$$

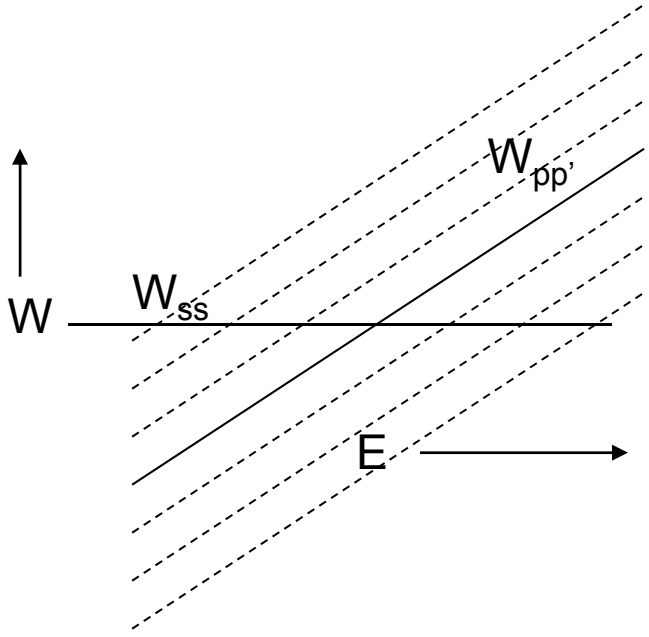

Since the cross section is proportional to the avoided crossing (at any R), the cross section for the m photon assisted collision Is given by

$$\sigma_m = \sigma\left|J\left(\frac{kE_{MW}}{\omega}\right)\right|$$

At finite R there are avoided crossings

where σ is the cross section in the absence of a microwave field.

Plot of the expected cross sections for 0, 1, 2, 3 photon resonances

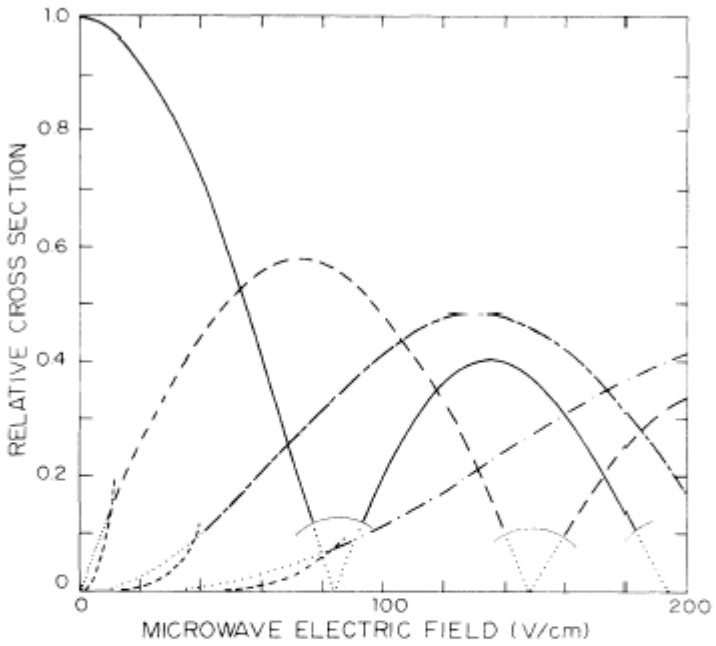

FIG. 19. Theoretical cross-section variation vs microwave field amplitude corresponding to the experimental data of Fig. 9. Strong-field regime, cross sections: $(0,0)^0$ (——), $(0,0)^1$ (— — —), $(0,0)^2$ (— - — -) and $(0,0)^3$ (— · — · —). Parts of curves where the strong-field-regime theory is not valid are dotted lines. Weak-field-regime cross sections are represented by short dashed lines for the processes $(0,0)^1$, $(0,0)^2$, and $(0,0)^3$.

This model gives the calculated curves.

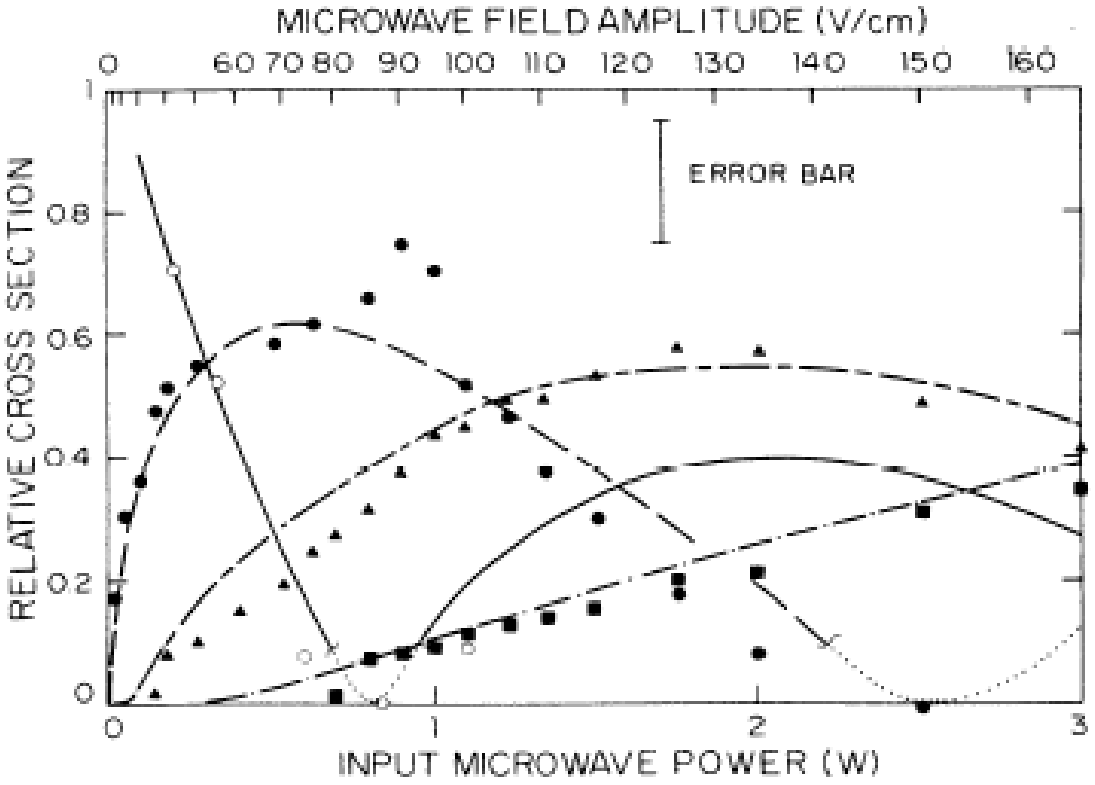

Similar experiments were done with velocity selected beams with K atoms with frequencies 1000 times lower.

K 29s + 27d→29p + 28p

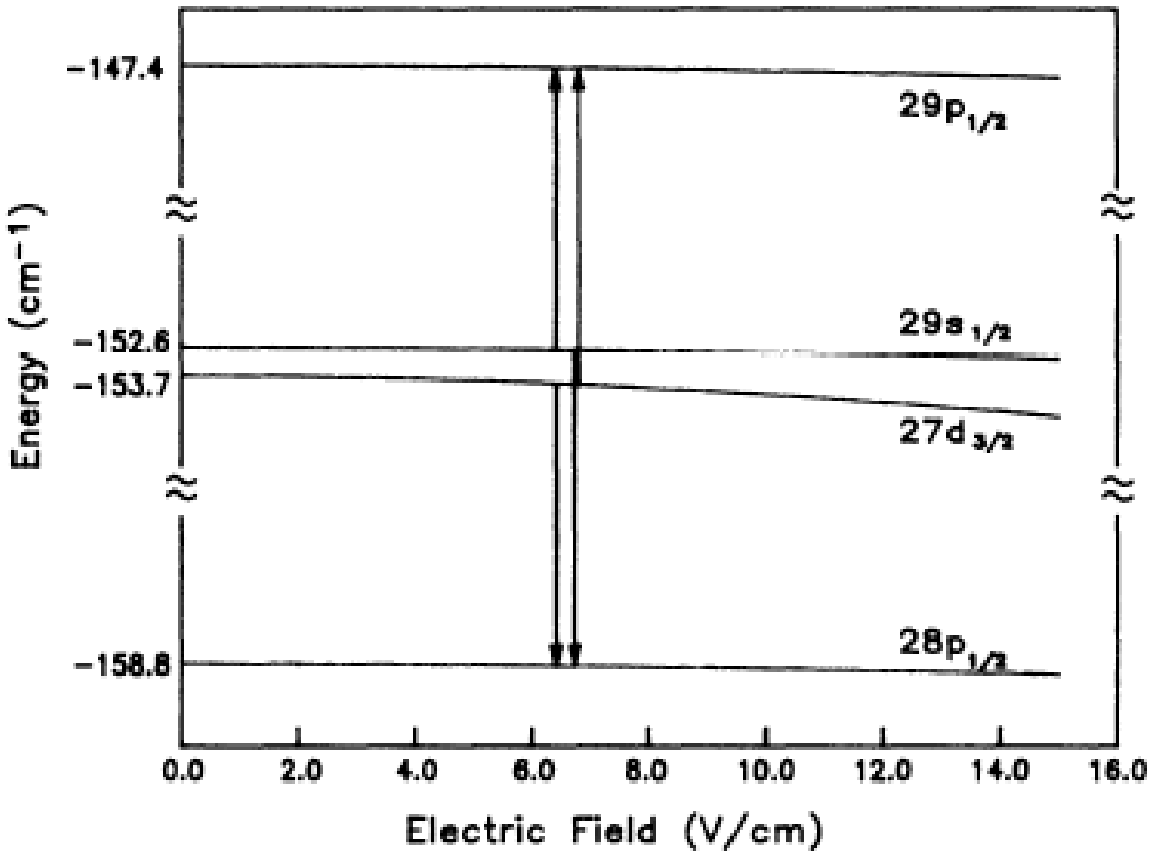

In this case it is the initial state which has the Stark shift.

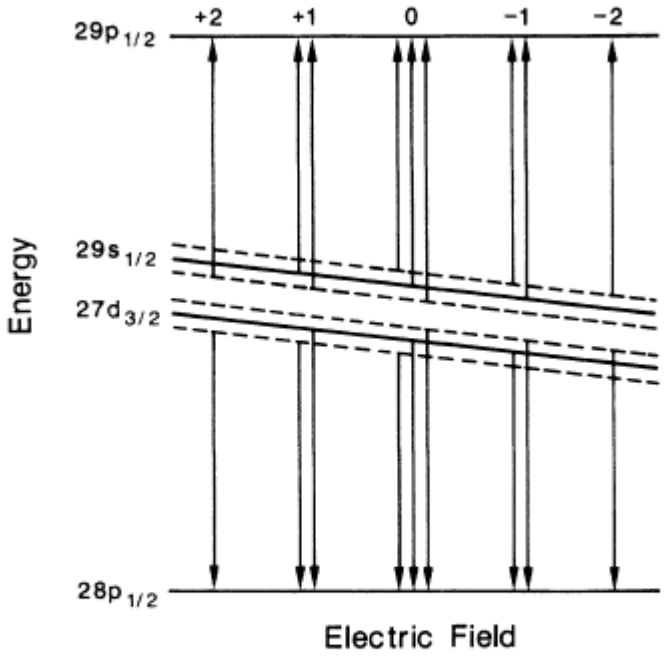

FIG. 2. Energy-level diagram of the K states in the presence of an oscillating electric field showing the additional sideband states and sideband resonances predicted by the Floquet theory. The numbers at the top label the sideband resonances according to how many rf photons are emitted by the atomic system for a radiatively assisted collision at that value of static electric field.

We have considered collisions in the combined static and rf fields

$$E(t) = E_S + E_{rf} \cos \omega t$$

We have considered applying frequencies high compared to the linewidths of the collisional resonances, or there are many microwave or rf cycles during the collision.

At the other extreme the rf field varies slowly compared to the duration of the collision. In this case the static field at which the resonance appears satisfies

$$E_0 = E_S + E_{rf} \cos \omega t$$

$$E_S = E_0 - E_{rf} \cos \omega t = E_0 - E_{rf} \cos \phi$$